EARTH SCIENCE AND RESOURCE ENGINEERING
www.csiro.au

Chemical Tracer Partition Coefficients for CCS

Matthew Myers, Tara La Force, Cameron White, Bobby Pejcic, Linda Stalker and Andrew Ross

March 22, 2013

CSIRO Report # EP142797

ANLEC R&D Project 3-1110-0125 Fundamentals of tracer applications for CO_2 Storage

Copyright and disclaimer

Important disclaimer

Contents

Figures

Tables

Acknowledgments

The authors wish to acknowledge the financial assistance provided through Australian National Low Emissions Coal Research and Development (ANLEC R&D), financial assistance from CSIRO Petroleum and Geothermal Portfolio and data provided by the CO2CRC. ANLEC R&D is supported by the Australian Coal Association Low Emissions Technology Limited and the Australian Government through the Clean Energy Initiative.

Executive Summary

The primary aims of this project are to establish general methodologies for determining supercritical carbon dioxide/water partition coefficients for chemical tracers and to determine these in a series of laboratory experiments for a variety of chemical tracers relevant to CCS. There is a general lack of information on these partition coefficients and often octanol/water and/or air/water partition coefficients are used as substitutes in simulations of tracer behaviour. However, supercritical carbon dioxide/water coefficients are necessary for both planning tracer field trials and accurately interpreting observed tracer behaviour. In the context of a monitoring and verification program for a CO_2 storage project, an accurate interpretation of tracer results is critical for determining whether leaking from the storage reservoir is occurring thus demonstrating a potential containment breach. To demonstrate the rationale for this project a review of known partition coefficients for chemicals of relevance to CCS as tracers is given. This review confirms that there is a general lack of data on supercritical carbon dioxide/water partition coefficients. The chemical thermodynamics governing the partitioning process is discussed and the general theory and experimental protocol for determining supercritical carbon dioxide/water partition coefficients is given. The specific methodologies implemented in this project for determining these coefficients for reactive ester tracers (propylene glycol diacetate, triacetin and tripropionin) and inert gas tracers (xenon, krypton, R134a, sulphur hexafluoride and perdeuterated methane) is given alongside a comprehensive table of partition coefficients at various temperatures for these tracers. We have shown that temperature dependence of the partition coefficient correlates well with a van't Hoff type relationship (i.e. ln K vs. 1/T). These correlations provide considerable insight into the thermodynamics associated with the partitioning process and will enable the accurate simulation of these chemical tracers at any temperature within the studied range of temperatures.

Part I Chemical Tracers and Partition Coefficients

1 Chemical Tracers in CCS Projects

1.1 Introduction

It is important to review the current literature to obtain any relevant information that may have been published on tracer compound partition coefficients between supercritical (and other forms of) CO_2 and water (with or without added minerals). It has been noted by various researchers examining the potential use of tracer compounds in carbon storage projects that quantified partition coefficients are greatly lacking (Myers et al., 2012a). As such, the Commonwealth Scientific Industrial Research Organisation (CSIRO) has invested in new equipment designed to make these measurements for various tracer applications. This project aims to measure partition coefficients for tracers that have already been deployed at various carbon storage sites. For example, the CO2CRC granted the project access to use the tracer data set generated at the CO2CRC Otway Stage 1 and Stage 2B projects in Victoria. With quantified partition coefficients, it will be possible to provide better constrained interpretations of observed tracer data and contribute towards reducing uncertainty in model forecasting. The following is a short summary of particular chemical tracers applied to various recent CCS projects globally with the goal of identifying a set of tracers that will be characterised as a part of this study. This will serve to validate the usefulness of the results that will be generated by the laboratory experiments that comprise the main research component of this project. Furthermore, this study will focus exclusively on chemical tracers that are added to the formation during injection and will not examine naturally occurring tracers (i.e. chemical species already previously present in the formation mobilized as a result of CO_2 injection).

Predicting and understanding the behaviour of CO_2 is challenging due to its complex phase behaviour (i.e. CO_2 can exist in the subsurface as a liquid, gas, supercritical fluid or a solute in water depending on the physical/chemical conditions) and the wide range of possible trapping mechanisms (i.e. residual, solubility, structural and mineral). Commonly proposed storage scenarios involve pumping CO_2 into reservoir rock formations at depths greater than 800 metres, where the pressure/temperature typically exceeds the critical point of carbon dioxide (7.38 MPa, 31.1°C). Chemical tracers represent a complimentary reservoir characterisation and monitoring tool to alternative approaches such as geophysical measurements (e.g. time lapse seismic) and have been used extensively worldwide at carbon capture and storage (CCS) sites. The majority of tracer applications within CCS are related to either understanding the subsurface movement of carbon dioxide (Boreham et al., 2011; Freifeld et al., 2005; Underschultz et al., 2011; Vandeweijer et al., 2011), quantifying the trapping capacity (Zhang et al., 2011) or determining containment and leakage rates for monitoring and verification programs (Strazisar et al., 2009; Wells et al., 2010; Wells et al., 2007). Chemical stability, cost effectiveness, ease of detection, toxicity, injection/sampling protocols and subsurface behaviour, together dictate the choice of tracer for a particular application or scenario.

1.2 Tracers Relevant to the CO2CRC Otway Project and Frio Brine Projects

Perdeuterated methane (CD_4), krypton (Kr) and sulphur hexafluoride (SF_6) were used as tracer gases for the CO2CRC Otway Stage 1 Project (Boreham et al., 2011). The breakthrough of the injected CO_2 plume was identified by the presence of the tracer compounds, an increase in CO_2 concentration over background levels and a change in the $\delta^{13}C$ of the measured CO_2. From the available publications on this project, reservoir simulation of tracer behaviour within the relevant geological formations is currently lacking (Boreham et al., 2011; Jenkins et al., 2012; Underschultz et al., 2011). Although, some activity has been

directed at reservoir simulation of the results, a full synthesis has not yet been published. This can be partially attributed to a distinct lack of fundamental information on tracer behaviour (derived from laboratory based experiments) with which to develop accurate models. Also in this case, the effect of methane (both within the storage reservoir and as component of the injected gas which contains approximately 20% methane) on tracer behaviour adds additional complexity to the system and its effect is largely unknown. In this case, these uncertainties in the physical properties of the tracer compounds translate into uncertainty in the interpretation of the final observations.

For the Frio Brine Projects in Texas, various perfluorocarbons, SF_6, Kr and CD_4 were injected as tracers to detect CO_2 breakthrough in an interwell (injector/producer) configuration (Hovorka et al., 2006). For similar reasons as with the CO2CRC Otway Project, a detailed reservoir simulation of tracer behaviour has not been published. Although tracer injections were useful in the case of both the Otway and Frio Brine projects for limited/qualitative interpretations (i.e. determining breakthrough of injected CO_2), for other purposes such as monitoring for leaks into the atmosphere, knowledge of the partitioning behaviour between water and CO_2 under a variety of geological conditions is instrumental. As such an understanding of tracer behaviour in CO_2/CH_4 and water would not only be very helpful for modelling tracer behaviour for the Otway and Frio Brine field trials, it would also provide critical information for interpreting tracer behaviour in future projects. Furthermore, tracer partition coefficient often determines the suitability of a tracer for a particular application (e.g. for estimating sweep volumes, non-partitioning tracers are appropriate whereas partitioning/reactive tracers are not).

Table 1 summarises the application of particular chemical tracers at various CCS sites around the world including at the Otway and Frio Brine sites. Not surprisingly, inert tracers which include perfluorocarbons (e.g. perfluorocyclohexane, perfluoromethylcyclopentane), krypton, xenon, sulphur hexafluoride, R134a and deuterated methane are the dominant choices due to their limited interaction with the reservoir rocks and formation water. Tracers with reactive functional groups are much less common.

Table 1 Tracers Implemented at CCS Projects

Tracers (*tracers chosen for characterisation as part of this ANLEC project)	**CCS site / Application**
Sulphur hexafluoride*, perdeuterated methane* and krypton*	Otway Stage 1 / understanding the migration of a CO_2/CH_4 mixture between a producer 300 metres up-dip from an injector and the influence of a natural gas-water contact on mixing (Boreham et al., 2011; Underschultz et al., 2011)
Sulphur hexafluoride *, krypton*, perfluorocarbons (perfluoromethylcyclohexane, perfluorotrimethylcyclohexane, perfluoromethylcyclopentane, perfluorodimethylcyclohexane) perdeuterated methane*	Frio Brine I / understanding the migration of carbon dioxide between a producer 30 metres up-dip from an injector (Freifeld et al., 2005) Frio Brine II / CD_4 and other tracers were tested to understand evolution of a CO2 plume in an interwell configuration.
Perfluorocarbons (perfluorodicyclohexane, perfluorotricyclohexane and perflurodimethylcyclobutane)	West Pearl Queen / surface gas samples are taken to assess formation-to-surface CO_2 leakage rates (Wells et al., 2007)
Krypton* and xenon*	Otway Stage 2B / in a single-well “push-pull” test to determine residual CO_2 saturation (Zhang et

	al., 2011)
Perfluoromethylcyclopentane and perfluorodimethylcyclohexane	K12B/to understand the migration of CO_2 between wells in a compartmentalized field
Reactive esters (propylene glycol diacetate, triacetin and tripropionin) and their hydrolysis products*	Otway Stage 2B / in a single-well “push-pull” test to determine residual CO_2 saturation

2 Partition Coefficients and Review of the Literature

Partition coefficients describe the equilibrium behaviour of a given chemical species between two immiscible phases (e.g. oil/water and air/water). For sufficiently dilute solution conditions (i.e. the concentration of the chemical species in each phase is much lower than the solubility limit), it is defined as the ratio of the chemical concentrations in each of the two phases (Srebrenik and Cohen, 1976). As tracers are typically utilized at low concentrations (i.e. ppm or lower concentration), partition coefficients are essential for accurately characterizing their behaviour in multi-phase systems. Both theory and practice have demonstrated that partition coefficients often exhibit Arrhenius type temperature dependence (i.e. log K vs. 1/T where T is the thermodynamic temperature and K is the partition coefficient) (Bahadur et al., 1997; Moreira et al., 1993).

Octanol-water partition coefficients have been used extensively in understanding and predicting the bioaccumulation and environmental fate of organic species (Cronin et al., 2003). Henry's Law coefficients (otherwise known as air/water partition coefficients) have been used to understand the interaction of atmospheric chemicals with bodies of water (Rathbun, 2000).

For CCS projects, the two most dominant phases within the formation are typically supercritical CO_2 and water. However, there is currently limited fundamental information on the supercritical CO_2/water partitioning behaviour for organic compounds (see Table 2 for a list of reported values) (Timko et al., 2004). Notably, there is no existing supercritical CO_2/water partition coefficient data for any inert gases used in the referenced CCS tracer test applications. Furthermore, there are currently no reports of any of the compounds in Table 2 (where the partition coefficients have been measured for supercritical CO_2/water partitioning) being used as tracers for either CCS or oil and gas projects. Rather, other partition coefficients (namely air/water [Henry's] and octanol/water) are often used as parameters in modelling tracer behaviour. In particular, the EOS7C module in the TOUGH2 dynamic reservoir simulation software has a parameter for the inverse Henry's coefficients which is used to describe tracer partitioning behaviour between CO_2 and water (Oldenburg et al., 2004). Octanol and air have very different chemical properties than supercritical carbon dioxide and as such these alternative parameters may not be representative or indicative of actual subsurface behaviour (Zhang et al., 2011).

The overall aim of this project is to address this knowledge gap through a variety of laboratory based experiments with the goal of determining the partitioning behaviour for a variety of chemical tracers under a range of physical conditions. This will result in more accurate modelling and interpretation of tracer data leading to reduced risk and uncertainty for site characterisation, insurance/permitting, well drilling/operation and monitoring/verification assessments. Generally this lack of fundamental information on tracer behaviour has resulted on a reliance on other types of partition coefficient (as described above) potentially resulting in inaccuracies or flaws in the interpretation of chemical tracer data.

Clearly there is a need to determine the partition coefficients of tracers in regards to their partitioning behaviour between supercritical CO_2 and H_2O or formation fluids for CCS projects. An estimation technique has been achieved (Fredenslund et al., 1975; Magnussen et al., 1981) for determining octanol/water partition coefficients uses structure activity relationships (SARs), which involves assigning a "contribution value" to chemical bonds and functional groups present in a molecule and summing these to obtain a partition. Although SARS has been used extensively, there is uncertainty in whether these estimates are sufficiently accurate for certain applications (Renner, 2002). Timko et al. (2004) measured the supercritical CO_2/water partition coefficients for a variety of organic compounds (e.g. aldehydes, ketones, esters, halides, phenols, alkanes and aromatic hydrocarbons) and showed that there is no adequate correlation with octanol/water partition coefficients, where the values are known for a much larger number of compounds (Haynes, 2011; Timko et al., 2004). They also looked at correlations with solubility parameters

(e.g. Hansen solubility indices) and other solvent/water partition coefficients (e.g. carbon disulfide/water) and found that none of these methods were sufficient for prediction. Currently, the limited data of partition coefficients precludes the development of even a rudimentary SARs type method for predicting supercritical CO_2/water partition coefficients. Consequently, in order to accurately model subsurface partitioning behaviour, an appropriate experimental protocol must be designed and conducted to actually determine the supercritical CO_2/water partition coefficients for relevant tracers.

Table 2 List of Known Supercritical CO2/Water Mole-Fraction Based Partition Coefficients in the Literature (from Timko et al. 2004 and references therein)*

Compound	Partition Coefficient	Compound	Partition Coefficient
Acetophenone	48.5 ± 4.6	Propiophenone	121 ± 13
Benzaldehyde	39.1 ± 3.7	Propylbenzoate	1050 ± 220
Bromobenzene	1090 ± 100	Tetrahydrofuran	8.5 ± 1.0
3-buten-2-one	7.8 ± 1	Toluene*	1200 ± 250.5
Chlorobenzene	1140 ± 110	Acetylacetone	3
Cyclohexane	4900 ± 600	Aniline	2.1
Cyclohexene	1900 ± 300	Benzene	2756
Cyclopentene	1400 ± 180	Benzoic acid	1.3
Ethylbenzoate	550 ± 100	Benzyl alcohol	1.9
Fluorobenzene	770 ± 150	Caffeine	0.15
Hexane	9000 ± 3000	2-chlorophenol	14
2-methoxyacetophenone	47.3 ± 4	4-chlorophenol	3
3-methoxyacetophenone	84.0 ± 7	Cyclohexanone	41
Methylbenzoate	205 ± 21	1,2–dichloromethane	154
Naphthalene	347	2,4–dichlorophenol	70
2-nitrophenol	80	2,4–dichlorophenoxacetic acid	0.1
4-nitrophenol	0.2	2,4–dimethylphenol	10.7
Parathion	18.3	Hexafluoroacetylacetone	0.7
Pentachlorophenol	80	2–hexanone	118
Phenol	1	3–methyl–4–chlorophenol	6
Salicylic acid	0.3	2-methyl-4,6-dinitrophenol	55
1,1,2,2-tetrachloroethane	84	2-methyl-5-hexyloxymethyl-8-	500
2,3,4,5-tetrachlorophenol	15	3-methylphenol	4
1,1,2-trichloroethane	28	Vanillin	1.5
2,4,6-trichlorophenol	150		

* Errors associated with partition coefficients have been added to the table where available. Partition coefficients were determined at 300 K at a variety of densities (or pressures). Mole-based partition coefficients are used as they are invariant with respect to density.

2.1 Currently Known Information on the Partitioning Behaviour of Inert Gas Tracers

Unfortunately, as mentioned earlier, there is a complete lack of data available for the supercritical CO_2/water partition coefficients for inert gas tracers. Consequently Henry's Law coefficients have been used instead of supercritical CO_2/water partition coefficients as input parameters in reservoir simulations

to characterise the subsurface partitioning behaviour of krypton and xenon (Zhang et al., 2011). Henry's Law coefficients have been determined for sulphur hexafluoride from 25 °C to 230 °C (Mroczek, 1997), krypton from 0 °C to 75 °C (Wilhelm et al., 1977), xenon from 0 °C to 75 °C (Wilhelm et al., 1977), R134a from 0 °C to 60 °C (Zheng et al., 1997) and perdeuterated methane from 12 °C to 52 °C (Gomes and Grolier, 2001) (see Table 3). These studies show that for these compounds, as expected, there is generally Arrhenius type temperature dependence. Furthermore, octanol-water partition coefficients have been determined for a very large number of non-gaseous chemical compounds (Haynes, 2011). A search of the literature has revealed that information on the octanol/water partitioning behaviour of many relevant fluorinated organic compounds (e.g. R134a and most perfluorocarbons) is also not currently available presumably due to their low solubility. It seems then that there is a distinct lack of data regarding the octanol/water partitioning behaviour of inert tracers as well. Given that the behaviour of tracer compounds from both of these classes will need to be interpreted for a number of geosequestration projects and are an important indicator of the effectiveness of a site for CO_2 storage, it is critical that the behaviour of these tracers in the conditions present in typical underground storage reservoirs is understood. Obtaining the partitioning behaviour over relevant geological pressures and temperature regimes for supercritical CO_2/water interfaces is therefore an important step in developing this understanding.

Table 3 Temperature Dependence of Henry's Coefficients for Inert Gas Tracers. Data amalgamated from (Mroczek, 1997, Wilhelm et al., 1977 and Gomes and Grolier, 2001.

Compound	Temperature (°C)	Henry's coefficient (MPa)
Krypton	0	663
	20	1150
	40	1850
	60	2830
	75	3760
Xenon	0	1250
	20	2010
	40	3040
	60	4380
	75	5600
R134a	5	155
	35	454
	65	823
CD_4	11.7	0.0640
	25	0.0424
	35	0.0733
	44.5	0.0528
	51.2	0.0874
SF_6	25	22900
	50	34900
	75	42200
	100	43500
	125	40100
	150	33900
	175	27200
	200	20700

	225	15500
	230	14600

2.2 Currently Known Information on the Partitioning Behaviour of Reactive Ester Tracers

For several years, we have been developing a class of reactive ester tracers capable of quantifying the residual carbon dioxide saturation in a formation and have determined the supercritical CO_2/water partitions coefficients for propylene glycol diacetate, triacetin, tripropionin and their hydrolysis products (Myers et al., 2012b). The partition coefficients were determined at the reservoir temperature and pressure intended for the CO2CRC Otway Stage 2B "Residual Saturation and Dissolution Test" (Table 4), where they have been recently utilised in the field as part of a larger test sequence (Paterson et al., 2010; Zhang et al., 2011). However, to extend the utility of these tracers to other field trails, further tests need to be performed over a larger range of geologically appropriate pressures and temperatures.

Table 4 Supercritical CO_2/water Partition Coefficients for Reactive Ester Tracers at 62 °C

Compound	Partition coefficient based on mole fraction of solute in solvent, k_i^x	Partition coefficient based on concentration at 15 MPa (similar PT conditions to Otway Stage 2B), k_i
Propylene glycol diacetate	54.5 ± 5.3	8.77 ± 0.86
Propylene glycol monoacetate 1	1.04 ± 0.12	0.167 ± 0.019
Propylene glycol monoacetate 2	9.79 ± 2.22	1.57 ± 0.36
Triacetin	27.7 ± 5.6	4.46 ± 0.90
Diacetin 1	0.837 ± 0.214	0.135 ± 0.034
Diacetin 2	0.769 ± 0.107	0.124 ± 0.017
Monoacetin 1	0.876 ± 0.272	0.141 ± .044
Monoacetin 2	0.163 ± 0.057	0.0263 ± 0.0093
Tripropionin	313 ± 58	50.3 ± 9.3
Dipropionin 1	5.09 ± 0.85	0.820 ± 0.137
Dipropionin 2	4.83 ± 1.06	0.778 ± 0.170
Monopropionin 1	8.72 ± 1.64	1.40 ± 0.26
Monoproprionin 2	0.349 ± 0.089	0.0562 ± 0.0143
Acetic acid	0.914 ± 0.256	0.147 ± 0.041
Propionic acid	1.50 ± 0.60	0.241 ± 0.097
Glycerol	[a]	[a]
Propylene glycol	[a]	[a]

[a] Glycerol and propylene glycol were not detected in the supercritical carbon dioxide phase. This is presumably due to their low solubility in supercritical carbon dioxide

3 Conclusions

In order to successfully determine the partitioning behaviour of chemical species in the subsurface environment, the methodology used for determining partition coefficients for tracers must be accurate and robust (Renner, 2002). In the next part, the thermodynamics of the partitioning process will be discussed and several methodologies for determining the supercritical CO_2/water partition coefficients will be presented (Ramachandran et al., 1996; Robbins et al., 1993).

Part II Partition Coefficients: Thermodynamics and Experimental Methods

1 Experimental Methods for Determining Tracer Partition Coefficients

Phase partitioning is a fundamental tracer property dictating subsurface behaviour. As such, tracer partition (or distribution) coefficients are required to correctly interpret tracer field results and for accurate reservoir simulations. Currently, there is lack of information on tracer partition coefficients between supercritical CO_2 and water. Due to this, in reservoir simulations of tracer behaviour, air/water (Henry's coefficients) or octanol/water partition coefficients are frequently substituted potentially leading to invalid predictions and large errors in estimates of reservoir properties. This project aims to address this lack of data through a program of laboratory experiments with the primary aim of determining these partition coefficients for a number of chemical tracers.

This part primarily consists of:

- A discussion of the thermodynamics related to distribution (or partition) coefficients
- A technical description of the general experimental methods that can be used to determine supercritical CO_2/water partition coefficients
- A summary of the tracer distribution coefficients that were? determined as part of this project

1.1 Thermodynamics

Distribution (or partition) coefficients are concerned with the equilibria of chemical species between two or more phases. For systems where there are no external force fields or internal barriers, this is formally defined as equivalency of the pressure (P), temperature (T) and chemical potential (μ) across the phases. Given pressure and temperature equivalency between phases, the partitioning behaviour of chemical species between phases is associated with the chemical potentials.

Generally, for a particular species *i* in phase *j*, the chemical potential is given by

$$\mu_i^j = \underline{\mu}_i^j + RTln\, a_i^j$$

where $\underline{\mu}$ is the chemical potential at a reference state, *R* is the gas constant and *a* is the activity. For the case of one component in two phases and equal temperature and pressure for the two phases, the equilibrium conditions reduces to

$$\underline{\mu}^1 + RTln\, a^1 = \underline{\mu}^2 + RTln\, a^2.$$

The activity is defined as

$$a^j = x^j \gamma^j$$

where *x* is the mole fraction and *γ* is the activity coefficient in each of the two phases. At dilute conditions (i.e. concentrations typically present for tracers and well below the solubility) the activity coefficient becomes constant and can be incorporated into the chemical potential (i.e. μ). The equilibrium condition becomes

$$\underline{\mu}^1 + RTln\, x^1 = \underline{\mu}^2 + RTln\, x^2.$$

Rearranging this gives the distribution coefficient as

$$K = \frac{x^2}{x^1} = e^{\frac{\mu^1 - \mu^2}{RT}}$$

with its temperature dependency (commonly known by the Arrhenius equation). There are several different ways of representing the distribution coefficient (e.g. the TOUGH2 reservoir simulator uses

inverse Henry's coefficient with units of Pa^{-1}, Eclipse and UTCHEM uses the dimensionless ratio of tracer concentration in two phases). For simplicity, this project will focus on the dimensionless distribution coefficient (i.e. ratio of the equilibrium concentrations in each of the phases), which can be easily converted to other forms through unit conversions and is the basis for thermodynamic equilibrium condition given above.

1.2 High-pressure/temperature experimental apparatus and sampling protocols

Recently, we reported a detailed description of the experimental apparatus to determine distribution coefficients for reactive ester tracers between supercritical carbon dioxide and water (Myers et al., 2012c). In summary, a high pressure/temperature rated container is filled with carbon dioxide and water. Liquid CO_2 is injected into the container using a high pressure syringe pump and the temperature and pressure are adjusted by varying the amount of carbon dioxide/water and the container temperature. The sample volume between two 3-way valves is used to obtain samples (after the sample loop fluid equilibrates with bulk fluid) of the gas phase and the water phase. In the case of non-volatile tracers (e.g. reactive ester tracers), these samples are slowly released into a volume of solvent in a glass vial. For this project, we have made several modifications and improvements to this initial design. Firstly, a high pressure piston-type circulation pump has been added to decrease equilibration time and reduce sampling variation. This allows us to increase experimental throughput, sampling reliability and reduce equilibration related issues with the increased hydrolysis rate of the reactive ester tracers at higher temperature (e.g. above 80 °C). A sampling system for obtaining high pressure gas samples of volatile tracers (i.e. xenon) in carbon dioxide has been developed. A series of diaphragm valves rated for vacuum to high pressure are used to evacuate the sampling line and a high pressure/low volume sample vessel. After evacuation, the gas sample at container pressure is expanded using the three-way valves into the small volume sample vessel for subsequent gas chromatographic analysis.

An extensive search of the literature has identified three methods to determine the distribution coefficients:

1. Direct measurement of concentrations in a closed pressurised vessel of both the supercritical CO_2 and water phases (Timko et al., 2004).
2. Measurement in a closed pressurised vessel of only one phase (e.g. only CO_2) and varying the ratios of the phase volumes while keeping the amount of the partitioning chemical species constant in the vessel (Gossett, 1987; Hansen et al., 1993; Ramachandran et al., 1996).
3. Measurement in a closed pressurised vessel of only one phase (e.g. only CO_2) and varying the ratios of the phase volumes while keeping the initial concentration in one of the phases (e.g. water) constant in the vessel (Robbins et al., 1993).

1.3 Direct measurement of concentrations in two separate phases

Conceptually this is the easiest method for determining partition coefficients and requires only one experiment; however, in practice it may be very difficult to attain an accurate determination of the partition coefficient. This method requires independently determining the concentration of a chemical species in both the supercritical carbon dioxide phase and the water phase and the partition coefficient is simply the ratio of these concentrations. Gas chromatography/mass spectroscopy (GCMS) is typically the most general and accurate way to determine these concentrations. Despite being convenient, there are a number of issues related to using water samples in a GCMS, namely the large expansion volume of water during injection and column/detector intolerance for water. Complete extraction of polar compounds into an organic phase more suitable for GCMS can be very difficult. Furthermore, extraction into a gas phase using purging techniques is often incomplete for organic compounds with limited volatility and dissolved gases have a strong tendency to remain in water. The efficiency of extraction techniques from water is

often difficult to predict precluding the accurate determination of dissolved gas concentration in the water phase.

This method has been used to determine the supercritical water/carbon dioxide partition coefficients for a variety of organic compounds (Timko et al., 2004). For collecting gas phase samples, carbon dioxide is slowly bubbled through chilled acetone for efficient collection of volatile compounds. The water samples were diluted into acetone before injection into a GCMS; in this case, water is diverted from the detector before the analyte elution from the column. Using this technique, Timko et al. reports errors for the solute concentrations in both phases using GCMS are 5 to 15 % resulting in 10 to 30 % errors for the partition coefficient. We have used this method with several modifications recently to determine the partition coefficients for reactive ester tracers (Myers et al., 2012c).

The advantages and disadvantages to this method are summarized below:

Advantages:
Only a single experiment needs to be conducted
Only method applicable to reactive tracers
Method is not sensitive to the relative ratios of water and supercritical CO_2
Disadvantages:
Large error due to difficulty in determining concentrations in water phase
Not suitable for gaseous or non-volatile tracers
Reliable sampling from both water and gas phases can be problematic

This is the method that will be used in this project to determine the distribution coefficients for the reactive ester tracers (i.e. propylene glycol diacetate, triacetin and tripropionin) and their related hydrolysis products. To implement this method, 1 g of each of the reactive tracers will be dissolved in 1 L giving a concentration of 1 g/L. This solution will be injected into the container where an appropriate amount of CO_2 will be added with the high pressure syringe pump. After heating to the appropriate temperature, the pressure will stabilize when equilibrium is achieved. To ensure uniform mixing, the circulation pump (rate of 8 mL/min) will be operated for approximately 8 hours at the beginning of the experiment and for 8 hours prior to each set of samples obtained.

1.4 Measurement of concentration in one phase, varying volume ratio of two phases with total amount of solute kept constant

This method involves a series of separate measurements of tracer concentrations in one phase while varying the volume ratio of the two phases and keeping the total amount of solute constant (see Figure 1 for an example of an experimental design for this method) (Gossett, 1987). Using this procedure, it is necessary to only measure the tracer concentration in the supercritical CO_2 phase; as such, errors associated with measuring gas/volatiles concentrations in water are eliminated. For the series of experiments, the number of moles of solute is kept constant and is partitioned between two phases giving the mass balance relationship

$$n = n_1 + n_2$$

where n is the total number of moles of solute and n_1 and n_2 are the number of moles in each of the two phases. Thermodynamic equilibrium is assumed for each of the measurements giving

$$K = \frac{c_1}{c_2}$$

where K is the dimensionless distribution coefficient and c_1 and c_2 are the solute concentrations in each of the two phases. The mass balance then becomes

$$n = KV_1c_2 + V_2c_2$$

where V_1 and V_2 are the volumes of each the two phases. With the total volume

$$V = V_1 + V_2,$$

this becomes

$$n = K(V - V_2)c_2 + V_2c_2.$$

Rearrangement of this gives

$$\frac{1}{c_2V_2} = \frac{K}{n}\left(\frac{V}{V_2}\right) + \frac{1-K}{n}.$$

The distribution coefficient K is determined by plotting the experimental data (c_2 is derived from GC analysis of the corresponding sample) from each of the measurements in the form $1/c_2V_2$ versus V/V_2. A linear regression is performed on this data and the ratio A of the y-intercept and the slope is determined. The estimated distribution coefficient determined using this method is given by

$$K = \frac{1}{1+A}.$$

Figure 1 An example of the different liquid to headspace ratios used to determine H for a given tracer. Total volumes of each sample bottle are constant as well as the amount of tracer added.

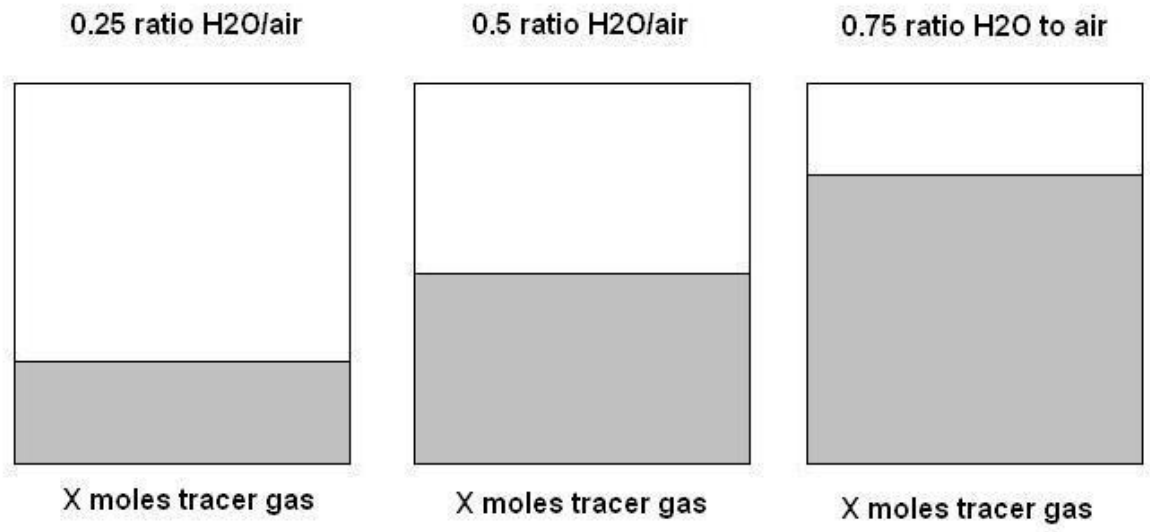

Ramanchadran et al. (1996) has shown using computer simulations that for the linear regression analysis detailed above to determine the distribution coefficient it is necessary to statistically weight the obtained data to obtain consistent results with minimal errors. This is due to the reciprocal nature of the plots generated for the linear regression. We assume that there is little error in the measurement of the water and CO_2 volumes and the measurement error is associated with the measurement of the concentration. In short, using the analysis above concentration measurements with the smallest error will have the largest errors in the linear regression analysis. This will cause inaccurate determinations of the distribution coefficient. To correct for this, each data point included in the linear regression should have a weighting of $(c_2V_2)^2$.

The advantages and disadvantages to this method are summarized below:

Advantages:

Use of multiple experimental runs with appropriate statistical weightings in a linear regression analysis can potentially lead to low errors in the estimation of the distribution coefficient

Only concentration in the gas phase need to be determined

Disadvantages:

This method is only applicable for inert (volatile or non-volatile) tracers

This method requires that the same amount of tracer is added for each measurement

The volume ratios of water and supercritical CO_2 need to be quantified for each measurement

This is the method that will be used in this project to determine the distribution coefficients for the inert gas tracer (i.e. krypton, xenon, perdeuterated methane, sulphur hexafluoride and R134a). To implement this method, a quantified amount of water is added to the container. Supercritical carbon dioxide is then added using the high pressure syringe pump and the container is heated to the desired temperature. The tracers are added using a series of sample loops (formed from adjoining two 3-way valves) in line with the circulation pump. To ensure uniform mixing and phase equilibration, the circulation pump (rate of 8 mL/min) is run for approximately 8 hours prior to sampling of the supercritical CO_2 phase into the high pressure sample containers.

1.5 Measurement of concentration in one phase, varying volume ratio of two phases while the initial concentration of solute in one of the phases is kept constant

This method involves a series of separate measurements of tracer concentrations in one phase while varying the volume ratio of the two phases and keeping the initial concentration in one of the phases constant (see Figure 2 for an example of an experimental design for this method) (Robbins et al., 1993). The concentration in this phase is a constant *c* and this phase has a volume V_2. The number of moles of solute in the container is given by

$$n = n_1 + n_2$$

where n_1 and n_2 are the number of moles in each of the two phases. As before, the thermodynamic equilibrium is assumed for each of the measurements giving

$$K = \frac{c_1}{c_2}$$

where *K* is the dimensionless distribution coefficient and c_1 and c_2 are the solute concentrations in each of the two phases. The mass balance then becomes

$$n = V_1 c_1 + \frac{V_2 c_1}{K}$$

where V_1 and V_2 are the volumes of each the two phases. With the total volume

$$V = V_1 + V_2,$$

this becomes

$$n = V_1 c_1 + \frac{(V - V_1) c_1}{K}.$$

Dividing by V_2 (or V-V_1) gives

$$c = \frac{V_1 c_1}{V_2} + \frac{c_1}{K}.$$

This can be rearranged to give

$$\frac{1}{c_1} = \frac{1}{c}\left(\frac{V_1}{V_2}\right) + \frac{1}{Kc}.$$

The distribution coefficient *K* is determined by plotting the experimental data from each of the measurements in the form $1/c_1$ versus V_1/V_2. A linear regression is performed on this data and the distribution coefficient is the ratio of slope and the y-intercept. Based on the work of Ramanchandran et al. (1996), the experimental data included in this linear regression should have a weighting of c_1^2.

Figure 2 A representation of the sample bottle setup for liquid tracers, the concentration of tracer in the liquid phase is the same in all bottles but the amount of moles varies.

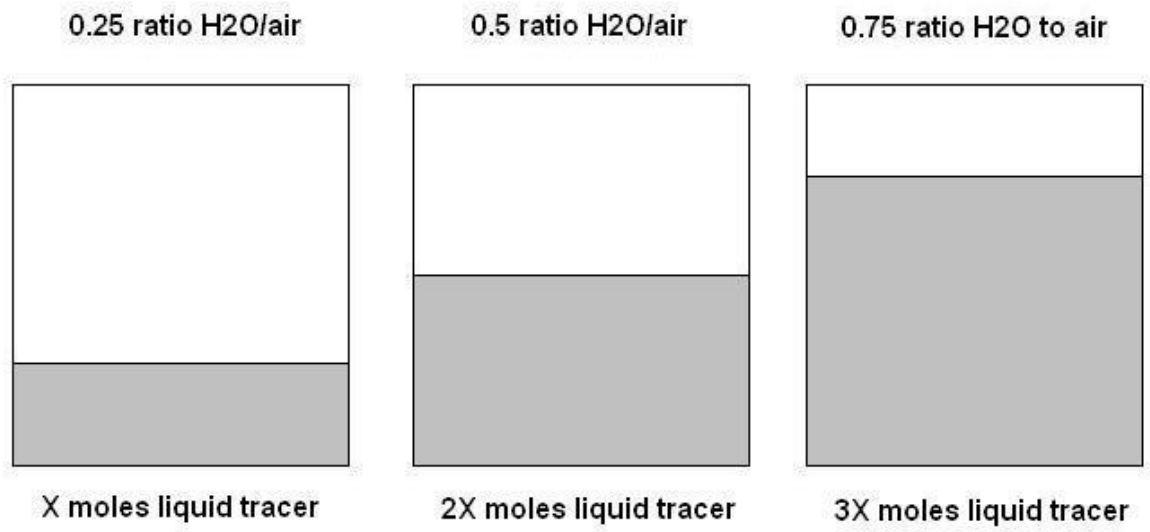

The advantages and disadvantages to this method are summarized below:

Advantages:
Use of multiple experimental runs with appropriate statistical weightings in a linear regression analysis can potentially lead to low errors in the estimation of the distribution coefficient
Only concentration in one of the phases need to be determined
Disadvantages:
This method is only applicable for inert (volatile or non-volatile) tracers
The volume ratios of water and supercritical CO_2 need to be quantified for each measurement

This method is ideal for non-volatile liquid inert tracers that readily dissolve in water and can be analysed with GC measurements from the water phase eliminating the complications associated with sampling from the supercritical CO_2 phase.

2 Scope of experimental projects determining tracer partition coefficients

Sulphur hexafluoride (SF_6), perdeuterated methane (CD_4) and R134a (or 1,1,2,2-tetrafluoroethane) were implemented as tracers at the Otway pilot site where CO_2 was injected into a depleted natural gas reservoir (Boreham et al., 2011; Underschultz et al., 2011). These tracers were used in an interwell configuration and confirmed the arrival of CO_2 at the observation well. Krypton, xenon and the reactive ester tracers were used at the CO2CRC's Otway Stage 2B Residual Saturation test in single-well "push-pull" tests (Myers et al., 2012c; Zhang et al., 2011).

Table 5 Scope of Tracer Partition Coefficient Studies

Tracers	Gas Composition	Temperature	Method of Measurement
Reactive esters (propylene glycol diacetate, triacetin and tripropionin)	100% CO_2	50, 70, 85, 100 and 120°C	Direct measurement of tracer concentration in both phases
Reactive esters	80% CO_2/20% CH_4	50, 70, 85, 100 and 120°C	Direct measurement of tracer concentration in both phases
Xe, Kr, SF_6, CD_4 and R134a	100% CO_2	59, 83, 100°C	Measurement of concentration in one phase, varying volume ratio of two phases with total amount of solute kept constant
Xe, Kr, SF_6, CD_4 and R134a	80% CO_2/20% CH_4	59, 83, 100°C	Measurement of concentration in one phase, varying volume ratio of two phases with total amount of solute kept constant

3 Conclusions

In order to successfully determine the partitioning behaviour of chemical species in the subsurface environment, the methodology used for determining distribution coefficients for tracers must be accurate and robust (Renner, 2002). As a result, we are currently testing and optimizing several new methodologies for determining the supercritical CO_2/water distribution coefficients (Ramachandran et al., 1996; Robbins et al., 1993). Our preliminary data shows that the CO_2/water distribution coefficient for the reactive esters and their hydrolysis products can be seen to decrease with increasing temperature. This indicates that a greater proportion of the tracer is remaining in the water phase as temperature escalates. With additional data at 70, 100 and 120 °C it will be possible to model the temperature dependence of the distribution coefficients for each tracer and establish a relationship. In the next part, we will report on the procedures used to determine supercritical CO_2/water partition coefficients for the reactive ester tracers. Furthermore, the partition coefficients themselves will be reported as well as the thermodynamic analysis of this data.

Part III Reactive Ester Tracer Partition Coefficients

1 Experimental Methods and Theory

1.1 Chemicals

Triacetin (glyercyl triacete, Aldrich, W200700, >98.5%, food grade), tripropionin (glyceryl tripropionate, Aldrich, W328618, food grade) and propylene glycol diacetate (Aldrich, 528072, >99.7%) were used as received for this study. Distilled water and 99.99% grade CO_2 (BOC) were used.

1.2 Apparatus and Experimental Methodology

A stainless steel (grade 316) container was designed to allow the experimental fluids to hydrolyse and partition at reservoir conditions (i.e. at elevated pressure and temperature). The container has a volume of 2.0 L with ¼" NPT female threading on both the top and base. Another similar container with a volume of 1 L has a separator installed and acts as a piston with a compression capacity of 930 mL. Using a high pressure syringe-type pump (with water as the compression fluid) and heating tape (with a PID type controller), pressure and temperature were maintained between 14 and 24 MPa (2050–3480 psi) and between 50 and 120^{o}C, respectively (see Figure 1). Both containers were equipped with H83 and FKB series Swagelok valves (rated to at least 27.5 MPa or 4000 psi at 120 °C).

For these studies, the system was filled with 1.5 L of distilled water and 1g (±0.05) g each of propylene glycol diacetate, triacetin and tripropionin. The container was pressurised with CO_2 (99.99% grade) to approximately 5 MPa (i.e. outlet pressure from a G-size gas cylinder), raised to the desired temperature with the heating tape and then further compressed to approximately 20 MPa by the piston pump before isolating the container using a valve. The supercritical CO_2/water fluid mixture was then recirculated overnight where it equilibrated. After the required temperature and pressure was attained the fluids were allowed to equilibrate and partially hydrolyse over a period of 2 to 20 days, which was dependant on the temperature conditions used. During this time, fluid samples were periodically acquired and analysed in pairs, one from the supercritical CO_2 phase (obtained from the top of the container) and one from the water phase (obtained from the base of the container).

The water sample was obtained by opening a valve attached to the bottom of the container and a second immediately adjacent needle valve, allowing the void volume (which was measured independently) between the two valves to fill up in the manner of a sample loop. After 1 hour (to allow for any equilibration) the first valve was closed and the water collected into a vial by opening the second valve. The sample loop was then flushed with chilled water to remove any residual sample into the vial. After sample collection, the sample loop was cleaned with acetone and then dried thoroughly with compressed air.

The sample from the supercritical CO_2 phase was collected in a similar manner. A valve attached to the top of the container was opened where the fluid was again allowed to equilibrate in the volume between the two valves, then the first valve was closed again isolating the sample loop. To

control the release of high pressure gas into a sample vial, a needle valve was used in combination with a ball valve to bubble the gas slowly through 10 mL of chilled water. The sample loop was then flushed with chilled water to remove any residual sample into the vial and then cleaned using the same protocol as the liquid sample. After collection, both samples were frozen before subsequent GCMS analysis.

Figure 3 Schematic of tracer setup including pumps, recirculation capacity and sampling ports

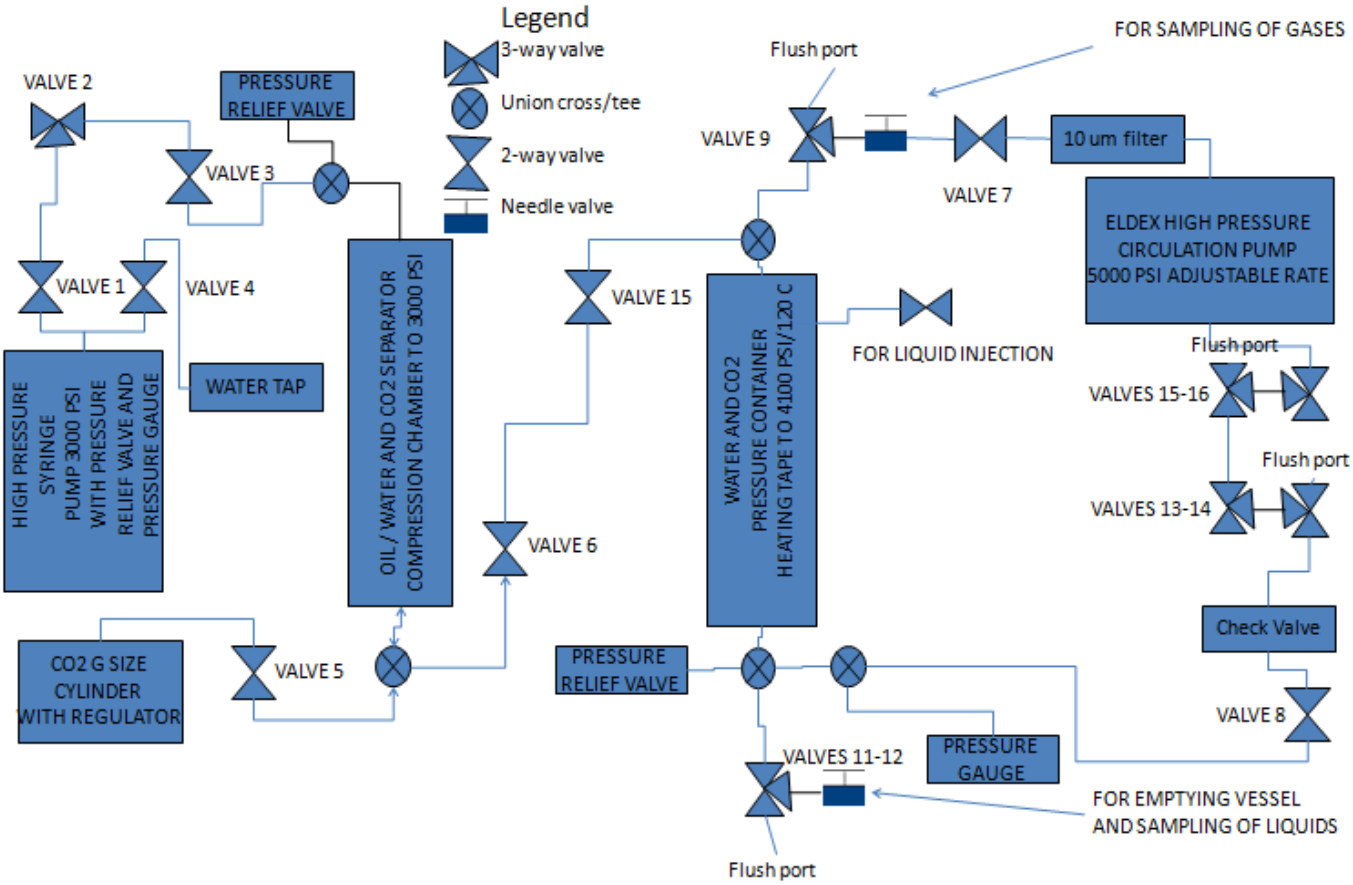

1.3 Preparation of Tracer Samples for GCMS Analysis

Two different GCMS columns and methods (detailed below) were used: the first aimed to accurately quantify the concentrations of the parent ester tracers (i.e. propylene glycol diacetate, triacetin and tripropionin) and the second aimed to quantify the concentrations of the different isomers of the hydrolysis alcohol products generated from the parent parent ester tracers (i.e. propylene glycol monoacetate diacetin, dipropionin). Prior to analysis, the samples were thawed to room temperature overnight and vigorously stirred prior to analysis. For the analysis of the parent parent ester tracers, some samples were diluted at either 5:1, 10:1 or 20:1 ratios prior to injection. For the analysis of the hydrolysis products, the samples were injected undiluted. Concentrations of standards used in constructing the calibration curves ranged from 2 μg/mL to 70 μg/mL. Compounds were identified by library matches and calibration standard peak areas were established using the automatic integration function followed by manual baseline adjustment

when required. Repeated (7 times) analysis of the same tracer sample gave a residual standard deviation of less than 8% in all cases.

1.4 GCMS Analysis of Parent Ester Tracers

Analysis was performed in split mode (split ratio 15:1) with an Agilent 6890 GC / Agilent 5973 inert MSD fitted with a RESTEK Stabilwax-DA column (30 m x 0.25 mm i.d., 0.25 µm film thickness). The carrier gas was helium with a constant column flow rate of 1.3 mL/min. Injection temperature was 250 °C and injection volume was 1 µL. The initial oven temperature was 70 °C which was ramped at 10 °C/min to 170 °C. The oven temperature was then held at 170 °C for 3 minutes before being ramped to 208 °C at 20 °C/min and held at that temperature for a further 3 minutes. The total run time was 17.9 minutes. The MSD conditions were typically: ionisation energy ~70eV, source temperature 230 °C and electron multiplier voltage ~ 1700V.

GCMS Analysis of Daughter Alcohol Tracers Generated by Hydrolysis of the Parent Ester Tracers
Analysis was performed in split mode (split ratio 2:1) with an Agilent 6890 GC / Agilent 5973 inert MSD fitted with a RESTEK Rtx-Bac1 column (30 m x 0.32 mm i.d., 1.8 µm film thickness). The carrier gas was helium with a constant column flow rate of 1.3 mL/min. Injection temperature was 250 °C and injection volume was 1 µL. The initial oven temperature was 70 °C which was ramped at 10 °C/min to 240 °C. The oven temperature was then held at 240 °C for 5 minutes. The total run time was 22.0 minutes. The MSD conditions were typically: ionisation energy ~70eV, source temperature 230 °C and electron multiplier voltage ~ 1700V.

Calculating Partition Coefficients

The method of determining the dimensionless partition coefficients for these parent esters involves the direct measurement of the chemical concentration in both the liquid and gaseous samples. The partition coefficients $K_{c/w}^{x}$ is defined as the ratio of the mole fractions in the supercritical carbon dioxide phase and the water phase and is calculated using

$$K_{c/w}^{x} = \frac{\frac{\mathrm{C_i}^{CO_2}}{\rho_{CO_2}}}{\frac{\mathrm{C_i}^{H_2O}}{\rho_{H_2O}}} \frac{MW_{CO_2}}{MW_{H_2O}}$$

where $K_{c/w}^{x}$ is the mole fraction basis dimensionless partition coefficient, $\mathrm{C_i}^{CO_2}$ and $\mathrm{C_i}^{H_2O}$ are the concentrations measured by GCMS in the supercritical carbon dioxide and water phases, ρ_{CO_2} and ρ_{H_2O} are the densities of the supercritical carbon dioxide and water phases (determined using the online calculator at http://webbook.nist.gov/chemistry/fluid) and MW_{CO_2} and MW_{H_2O} are the molecular weights of water and carbon dioxide. Utilizing this formula for a number of repeat experiments, the average partition coefficient and a standard error can be obtained for a variety of temperatures conditions.

2 Results and Discussion

As mentioned earlier, for the reactive esters, samples from both the water and supercritical CO_2 phase were taken in order to determine the amounts of tracer in each phase. GC analysis was then performed on each sample and after calculation performed on data to obtain the partition coefficients (Equations 1-3) the results for each tracer could be collated (Table 4).

$$Distribution\ coefficient = \frac{Concentration\ in\ supercritical\ CO_2}{Concentration\ in\ H_2O}$$

Where:

Concentration in supercritical CO_2 = concentration of tracer determined by GC / mass of CO_2 sampled

Concentration in H_2O = concentration of tracer determined by GC / mass of H_2O sampled

Consequently, this above equation can also be written as;

$$Distribution\ coefficient = \frac{\frac{[tracer\ in\ CO_2](g/cm^3)}{density\ CO_2(g/cm^3)}}{\frac{[tracer\ in\ H_2O](g/cm^3)}{density\ H_2O(g/cm^3)}}$$

The concentration of the tracers were determined from GCMS analysis while the density of the CO_2 and H_2O phases were calculated from literature tables utilizing the known temperature and pressure at the time of sampling. As most literature sources give the dimensionless distribution coefficient on a mole fraction basis, the density of CO_2 and H_2O need to be divided by their respective molecular weights.

$$Partition\ coefficient = \frac{\frac{[tracer\ in\ CO_2](g/cm^3)}{density\ CO_2(g/cm^3)}}{\frac{[tracer\ in\ H_2O](g/cm^3)}{density\ H_2O(g/cm^3)}} x \frac{MW\ CO_2}{MW\ H_2O}$$

For each tracer three separate samples were taken at time intervals spaced to ensure that a significant amount of hydrolysis had taken place. This allowed the partition coefficients to be calculated for the breakdown products of the tracers as well as the parent compounds at several stages along the hydrolysis chain to improve accuracy and robustness of the experiments. The total hydrolysis time was heavily dependent on the temperature, ranging from several weeks at 50^{o}C to several days at 120^{o}C.

In Table 1 below, we summarize the partition coefficient data that has been acquired to date. In instances where we have not reported a value this is due to very low concentrations measured in either the supercritical carbon dioxide phase and/or the water phase. Further experiments are currently underway to adjust hydrolysis conditions to maximize tracer concentrations.

Table 6 Dimensionless partition coefficient data for reactive parent ester tracers and their daughter hydrolysis products at varying temperatures

Tracer	Temperature °C	Average partition coefficient	Std Error
Propylene glycol	50	-	-
	70	0.64	0.15
	85	1.02	0.35
	100	0.96	0.16
	120	1.21	0.015
Glycerol	50	-	-
	70	-	-
	85	-	-
	100	0.71	0.21
	120	1.04	0.21
Propylene glycol diacetate	62	54.5	0.05
	70	18.1	0.10
	90	8.5	0.17
	100	5.8	0.13
	110	3.3	0.18
Triacetin	62	27.7	0.10
	70	8.2	0.07
	85	3.4	0.03
	110	1.1	0.03
	120	0.7	0.05
Tripropionin	62	313	0.09
	70	121	0.10
	85	29.1	0.15
	90	9.3	0.13
	110	7.2	0.17
Propylene glycol monoacetate 1	50	0.89	0.058
	70	1.02	0.13
	85	1.45	0.20
	100	1.18	0.14
	120	1.80	0.19
Propylene glycol monoacetate 2	50	0.74	0.082

	70	0.85	0.13
	85	1.34	0.17
	100	1.02	0.17
	120	1.64	0.19
Monoacetin 1	50	-	-
	70	0.56	0.32
	85	1.73	0.17
	100	0.38	0.099
	120	0.32	0.11
Monoacetin 2	50	-	-
	70	-	-
	85	-	-
	100	-	-
	120	-	-
Diacetin 1	50	0.61	0.033
	70	0.63	0.11
	85	1.12	0.19
	100	0.45	0.21
	120	0.55	0.14
Diacetin 2	50	0.59	0.026
	70	0.87	0.16
	85	1.02	0.13
	100	0.47	0.13
	120	0.68	0.16
Monopropionin 1	50	-	-
	70	0.60	0.21
	85	-	-
	100	0.48	0.012
	120	0.48	0.073
Monopropionin 2	50	-	-
	70	-	-
	85	-	-
	100	-	-
	120	-	-
Dipropionin 1	50	1.33	0.18

	70	1.78	0.052
	85	2.78	0.59
	100	0.90	0.14
	120	0.85	0.11
Dipropionin 2	50	1.61	0.21
	70	1.87	0.028
	85	2.76	0.41
	100	0.93	0.093
	120	0.86	0.24
Acetic acid	50	0.84	0.10
	70	1.74	0.25
	85	3.03	0.21
	100	3.95	0.16
	120	2.60	0.075
Propionic acid	50	1.08	0.36
	70	1.12	0.56
	85	2.50	0.26
	100	3.40	0.25
	120	1.88	0.072

In Figures 2 to 8, we have plotted the natural logarithm of the partition coefficient versus the reciprocal absolute temperature for a number of different chemical tracers. The data generated in these plots is fitted to the van't Hoff equation using a linear regression:

$$\ln K_{c/w}^{x} = \frac{-\Delta H}{RT} + \frac{\Delta S}{R}$$

where ΔH and ΔS are the enthalpy and entropy changes, respectively, associated with the partitioning process. This allows us to both estimate the enthalpy change and develop a correlation for predicting partition coefficients values over a range of temperatures. The results of the linear regressions of these plots are summarized in Table 2 below.

Figure 4 van't Hoff plot for propylene glycol diacetate

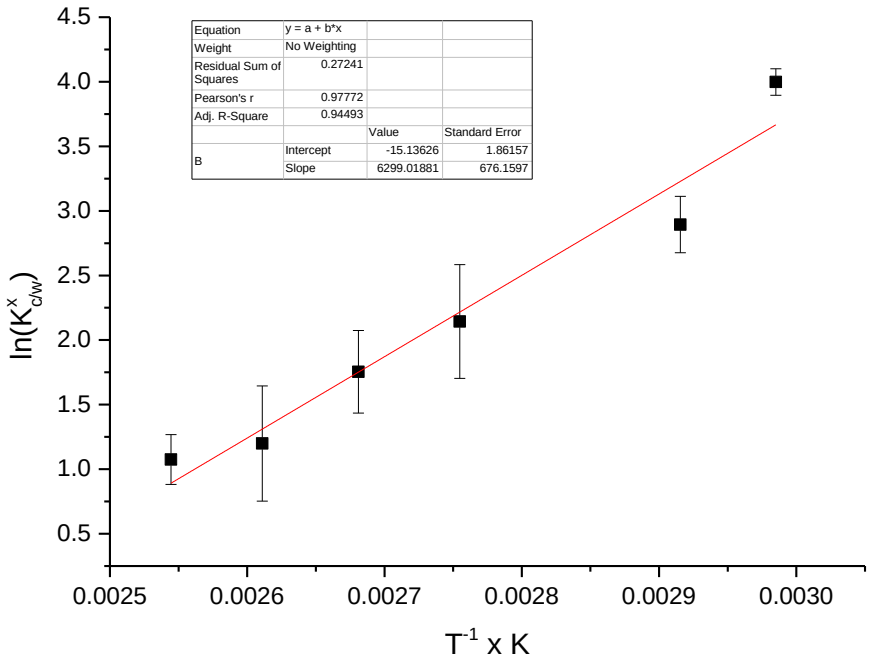

Figure 5 van't Hoff plot for triacetin

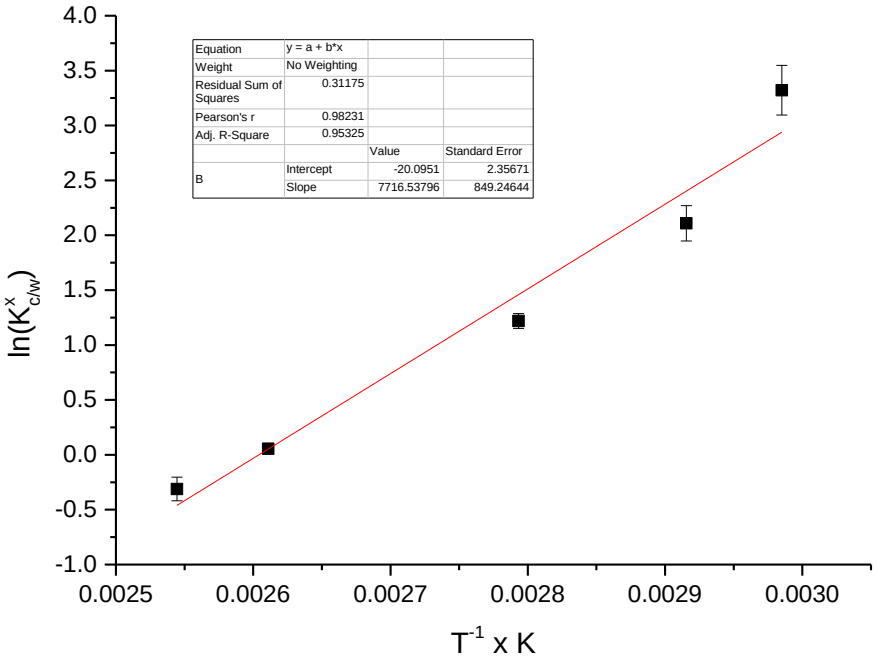

Figure 6 van't Hoff plot for tripropionin

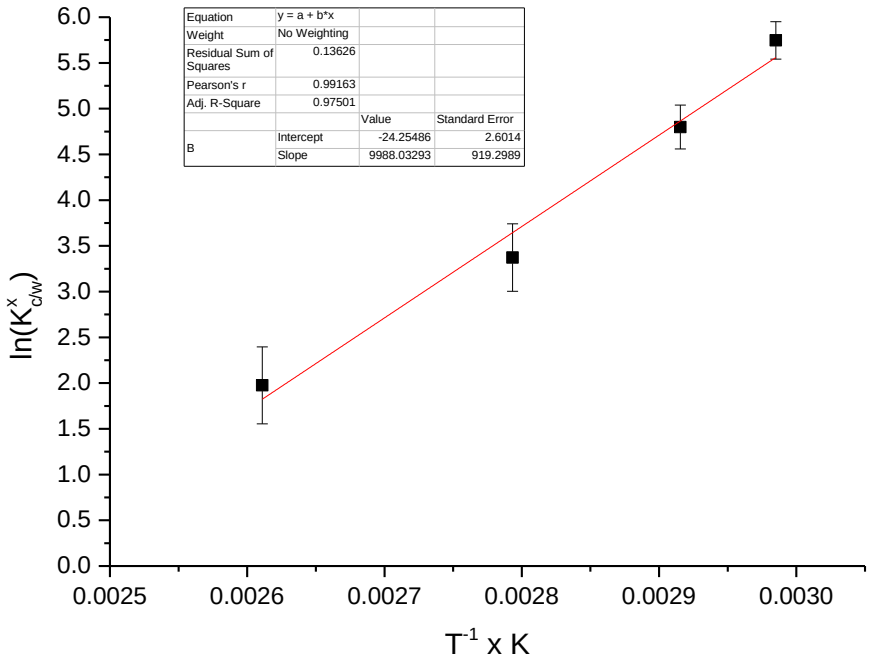

Figure 7 van't Hoff plot for propylene glycol monoacetate isomer 1

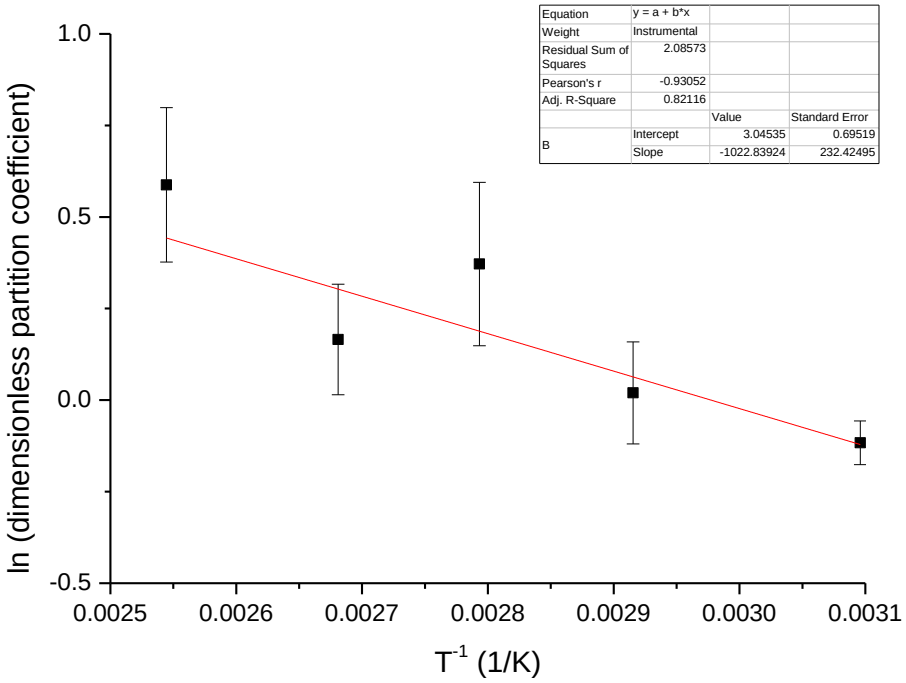

Figure 8 van't Hoff plot for propylene glycol monoacetate isomer 2

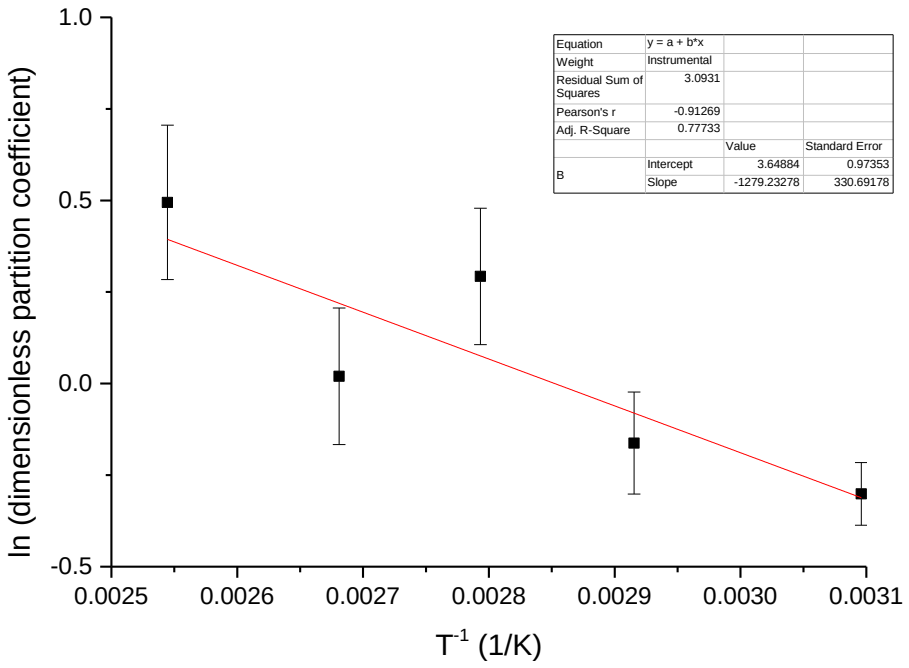

Figure 9 van't Hoff plot for dipropionin isomer 1

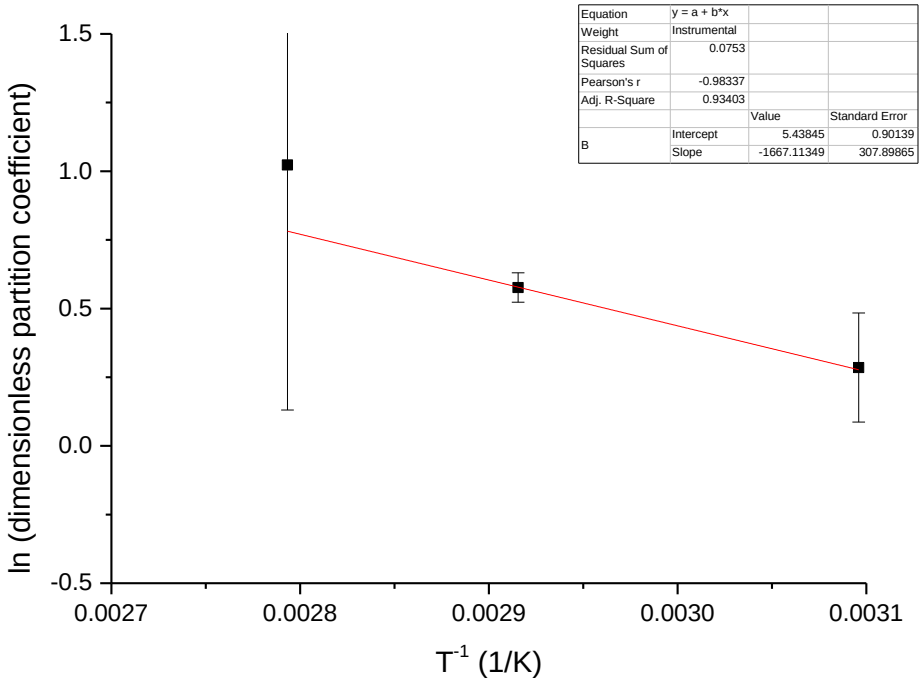

Figure 10 van't Hoff plot for dipropionin isomer 2

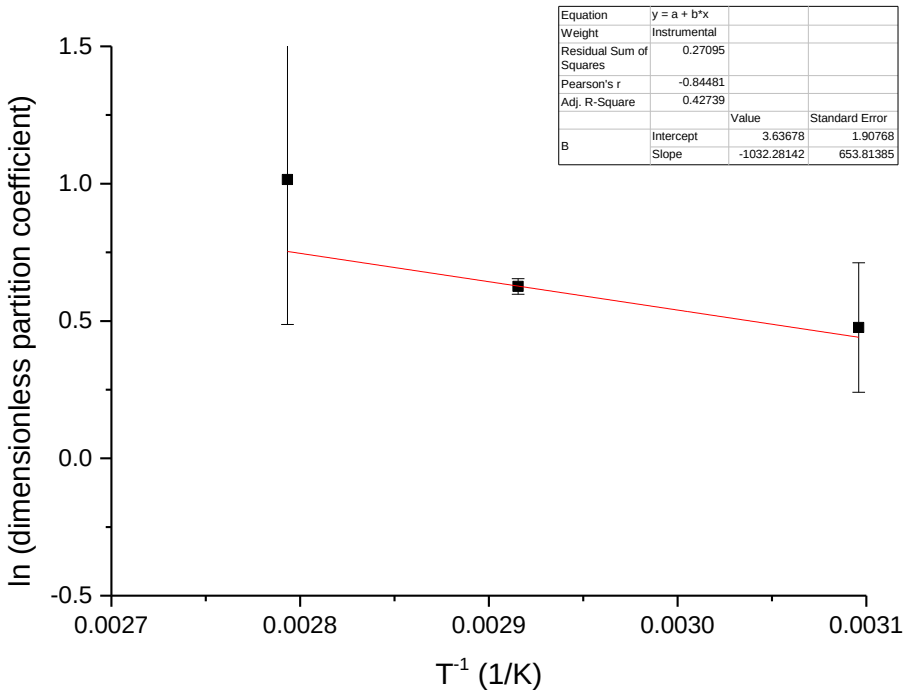

Table 7 The calculated enthalpies of selected tracers

Tracer	ΔH (kJ/mol)	Error
PGDA	- 52.3	5.6
Triacetin	- 64.1	7.1
Tripropionin	- 83.0	7.6
PGMA isomer 1	8.5	1.9
PGMA isomer 2	10.6	2.7
Dipropionin isomer 1	13.9	2.6
Dipropionin isomer 2	8.6	5.4

3 Conclusion

We have successfully determined partition coefficients for the parent parent ester compounds and their hydrolysis products under a range of temperature conditions. Furthermore, we have shown for several of these tracers that the temperature dependence of the partition coefficients follows a van't Hoff type equation.

Using the parent ester tracer data from Table 2, we have plotted enthalpy vs. number of carbons. There is a linear relationship between the number of carbon atoms and the enthalpy. This type of correlation is consistent with other work for octanol-water partition coefficients and can be useful to estimate the thermodynamic properties and partition coefficients of similar parent ester compounds.

Figure 11 Plot of enthalpy data vs. number of carbons for parent ester tracers

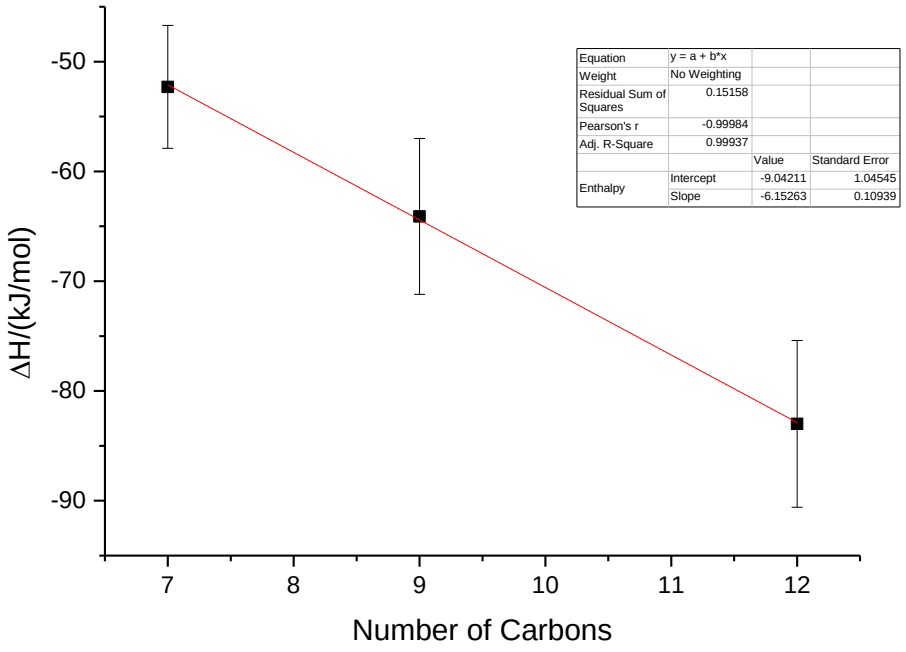

Part IV Inert Gas Tracer Partition Coefficients

1 Experimental Methods and Theory

1.1 Chemicals

A G size cylinder of 1% xenon, 1% 1,1,2,2-tetrafluoroethane, 1% krypton and 1 % sulfur hexafluoride mixture in carbon dioxide from Coregas and a lecture bottle of perdeuterated methane from Cambridge Isotope Laboratories were used as our source of chemical tracers for this study.

1.2 Apparatus and Experimental Methodology

Due to difficulties in the quantitative extraction and subsequent GC analysis of tracer gases in water, it was preferred that we developed a method which would circumvent the requirement to measure concentrations in both phases. As outlined earlier (Part II, Section 1.4), an experimental procedure was used where the amount of solute (i.e. tracer gas) is kept constant for the study while varying the volume of water to gas. Using this procedure, we can rely solely on the analysis of tracer concentrations in the supercritical CO_2 phase to determine partition coefficients.

A stainless steel (grade 316) container (with a measured internal volume of 1.750 L) with ¼" male NPT fittings at the top and bottom of the vessel was used for phase equilibration of tracer gas concentrations under reservoir conditions (i.e. at elevated pressure and temperature). Another similar container with a volume of 1 L has a separator installed and acts as a piston with a compression capacity of 930 mL. Prior to each experiment, the pressure vessels are dried clean with compressed air; following this the desired amount of distilled water is added. Using a high pressure syringe-type pump (with water as the compression fluid) and heating tape (with a PID type controller), CO_2 is added and the pressure and temperature were maintained between 140 and 180 bar and at 59 and 82^{o}C (to determine the effect of temperature on the partition coefficient). Both containers were equipped with Swagelok H83 and FKB series two-way and three-way valves (rated to at least 27.5 MPa or 4000 psi at 120 °C). An Eldex high pressure circulation pump (B100-S-2CE, up to 8 mL/min, rated to 5000 psi) was used to circulate supercritical CO_2 into the water phase overnight equilibrating the tracer concentrations. The gas sample loop is an interconnected 3-way valve (approximately 2 mL in volume) allowing for sample acquisition and loop purging. To ensure maximum representativeness of the gas sample, the circulation pump is put in-line with the gas sample loop. Tracers are injected using two similarly interconnected 3-way valves (one for tracer mixture from Coregas and the other for CD_4) in-line with the circulation pump. To ensure the same amount of tracer is used for each experiment, a low-pressure two-stage pressure regulator is used with each tracer loop and is purged by flowing tracer gas through the loop for each experiment. A vacuum manifold using Swagelok DS series valves (rated from vacuum to 241 bar) was attached to a 50 mL 316 SS sample cylinder and the sample loop outlet for the CO_2 phase of the pressure vessel. For each sample, the manifold and sample cylinder is evacuated prior to sampling. To obtain a gas sample, the sample loop is filled and the loop valves are closed. After attachment of the sampling manifold to the sample loop, the valve is opened and the sample is acquired by closing the valves. For each sample, the vessel pressure and temperature is recorded to allow for calculation of the water density and CO_2 density.

1.3 GCMS Analysis of Tracer Gases

Gas samples were sampled in a 50 mL stainless steel cylinder. The cylinder was attached to a vacuum manifold to evacuate from the septum to main valve port and then the gases were released to the vacuum manifold by opening the main valve slowly until the gases in the vacuum manifold reached atmospheric pressure. A gas tight syringe was used to withdraw 250 µL of gases from the septum port on the vacuum manifold for analysis. The gas concentrations were calculated by external standard calibration. Standard gas mixtures (1 and 10 ppm) were measured before the unknown samples were run to obtain a calibration curve. One of the standards was also measured normally at the end of the sequence of gas analysis as an unknown sample to make sure that there was no drift of the instrument. For CD_4 analysis, 1/10 dilution had to be made using 10 mL gas tight syringe and vacuum manifold because the CD_4 concentration in the samples was too high to be calibrated with our standards.

Trace gas analysis was performed on an Agilent GC (7890) interfaced with a high resolution Thermo DFS GC-MS system (electron energy 70eV; source temperature 280°C) tuned to 1000 resolution. CD_4, SF_6, krypton (Kr) and xenon (Xe) were analysed on a Varian PLOT fused silica column coated with molesieve 5A (CP7540; 50 m x 0.32 mm i.d., DF = 30 µm) and R134a was analysed on a Varian Pora^{TM} PLOT Q fused silica column (CP7551; 50 m × 0.32 mm i.d.). The head pressure of the column was set to 25 psi with a split flow of 23 mL/min. The GC Injector temperature was 250°C. The samples were run using a single ion monitoring (SIM) programme. Three experiments were written specifically for optimal analysis of CD_4, SF_6, Kr, Xe and R134a. The programme is listed below, along with the associated GC programmes and the diagnostic mass to charge ratios used:

1. Programme TraceGas_SF6_CD4 (0-12 min):
   This programme was performed using a two-section experiment with 12 min runtime. The GC oven temperature was isothermal 40 °C. SF_6 and CD_4 elute at ~2.3 min and 10.9 min respectively.
   Section 1(0-5 min): *m/z* 118.99147 (Lock mass), *m/z* 126.9541 (SF_6), *m/z* 130.99147 (Cali mass).
   Section 2 (5-12 min): *m/z* 18.01002 (Lock mass), *m/z* 20.0558 (CD_4), *m/z* 30.99188 (Cali mass).

2. Programme TraceGas_Kr_Xe (0-8 min):
   This programme was analysed using a one-section experiment with 8 min runtime. The GC oven temperature was isothermal 250 °C. Kr and Xe elute at ~4.1 min and 5.8 min respectively.
   m/z 83.9115 (Kr), *m/z* 99.99306 (Lock mass), *m/z* 130.99147 (Cali mass), *m/z* 131.9041 (Xe)

3. Programme TraceGas_R134A (0-10 min):
   This programme was analysed using a one-section experiment with 10 min runtime. The GC oven temperature was isothermal 100 °C. R134a elutes at ~7.6 min. *m/z* 51.00408 (Lock mass), *m/z* 83.0108 (R134a), *m/z* 99.99306 (Cali mass).

Tracers were calibrated by two certified standard gas mixture (~1 and ~10 ppm) from Coregas. 1 ppm standard gas mixture contains CH_4 (2.1 ppm), SF_6 (1.1 ppm), Kr (1.1 ppm), Xe (1.1 ppm), R134a (1.1 ppm), CD_4 (1.0 ppm) in helium. 10 ppm standard gas mixture contains CH_4 (21.2 ppm), SF_6 (10.7 ppm), Kr (11.0 ppm), Xe (10.8 ppm), R134a (10.6 ppm), CD_4 (9.8 ppm) in helium.

1.4 Determination of Inert Gas Tracer Partition Coefficients

The general method outlined in detail in Part II, Section 1.4 is used here to determine the supercritical CO_2/water partition coefficients for the inert gas tracers (i.e. krypton, xenon, sulfur hexafluoride, R134a and CD_4). To determine the supercritical CO_2/water partition coefficient, a series of experiments are conducted in which the volume of water is varied. At each volume, two gas samples are acquired and the results are averaged. For each experiment the amount of tracer gas is constant and given by $n = n_{water} + n_{CO_2}$ where n_{water} and n_{CO_2} is the amount of tracer gas in the water and CO_2 phases, respectively. The equilibrium expression is given by $K = \frac{C_{CO_2}}{C_{water}}$ where K is the partition coefficient and C_{water} and C_{CO_2} are the tracer concentrations in the CO_2 and water phases, respectively. Combining these expressions and multiplying the tracer concentration in each phase by the volume of each phase, the expression $n = C_{CO_2}V_{CO_2} + \frac{C_{CO_2}}{K}V_{water}$ is obtained. This can be rearranged to give $\frac{1}{C_{CO_2}V_{water}} = \frac{V_{CO_2}}{V_{water}}\left(\frac{1}{n}\right) + \left(\frac{1}{Kn}\right)$. By plotting the experimental data as $\frac{1}{C_{CO_2}V_{water}}$ vs. $\frac{V_{CO_2}}{V_{water}}$, a linear regression analysis will give a slope and y-intercept where the partition coefficient $K = \frac{slope}{y-intercept}$ can be estimated according to the above relationship.

2 Results and Discussion

As mentioned earlier, the volume for the water phase has been adjusted according to estimates of dissolved CO_2 and changes in water density due to pressure and temperature differences. For each series of experiments, a combination of 500 mL, 1000 mL, 1250 mL and 1500 mL of water was added to the pressure vessel. For each tracer at the two different temperatures (59 and 83 °C), either three or four samples were acquired and then subsequently analysed. This number of experiments is standard within the literature for determining partition coefficients (Atlan et al., 2006; Lau et al., 2010; Ramachandran et al., 1996). Generally, each regression analysis of the data gave a coefficient of determination R^2 greater than 0.99 (see Figures 12 to 21). From these regressions, the partition coefficient and associated error is given in Table 8. Estimates of partition coefficients are determined by the ratio of the slope to y-intercept from each linear regression. The errors are calculated based on a mathematical formulation for determining the approximate standard deviation for the ratio of two dependent random variables. The mathematical derivation of this approximation is available elsewhere (Atlan et al., 2006). This is a standard method that utilizes the first order Taylor series approximation of the ratio. The standard deviation is calculated from the second term of this approximation and utilizes the covariance matrix associated with each linear regression.

Figure 12 $1/C_{CO2}V_{water}$ vs. V_{CO2}/V_{water} plot for sulphur hexafluoride at 59 °C

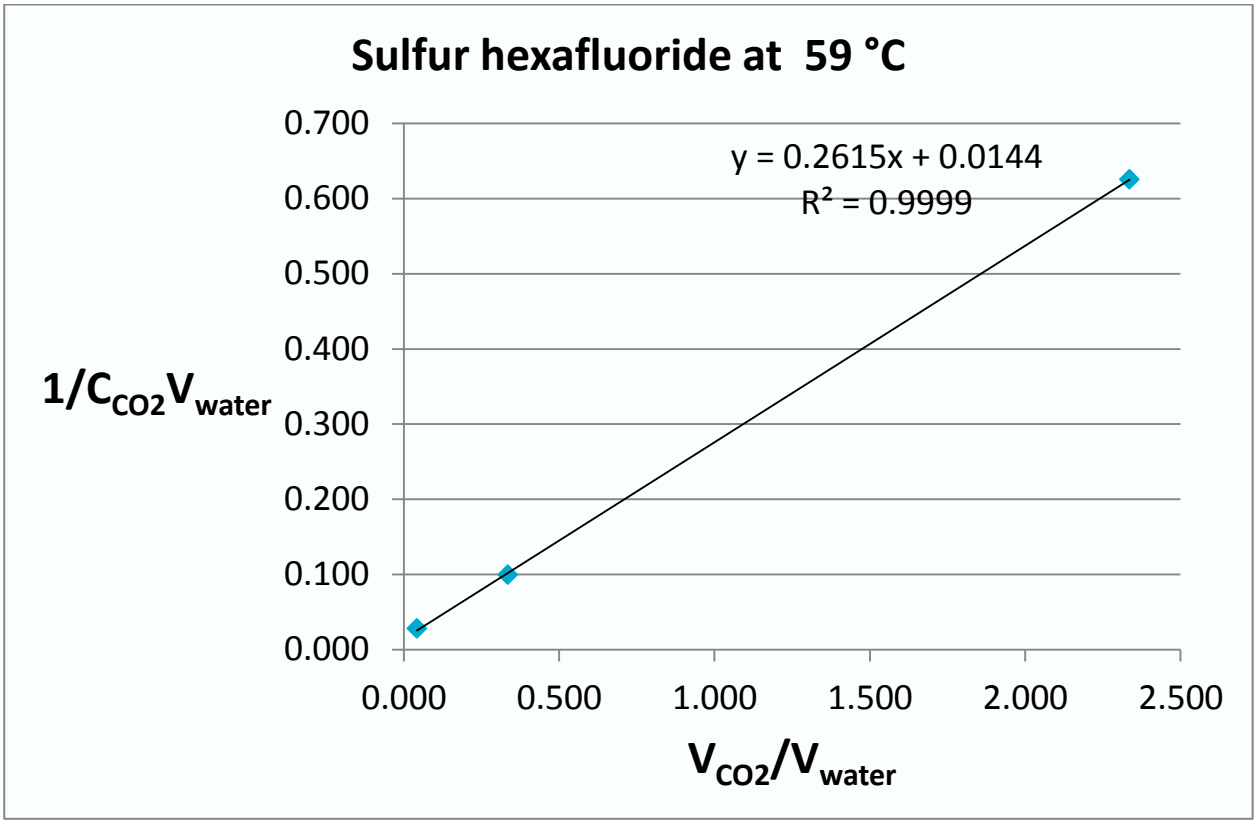

Figure 13 $1/C_{CO2}V_{water}$ vs. V_{CO2}/V_{water} plot for sulphur hexafluoride at 83 °C

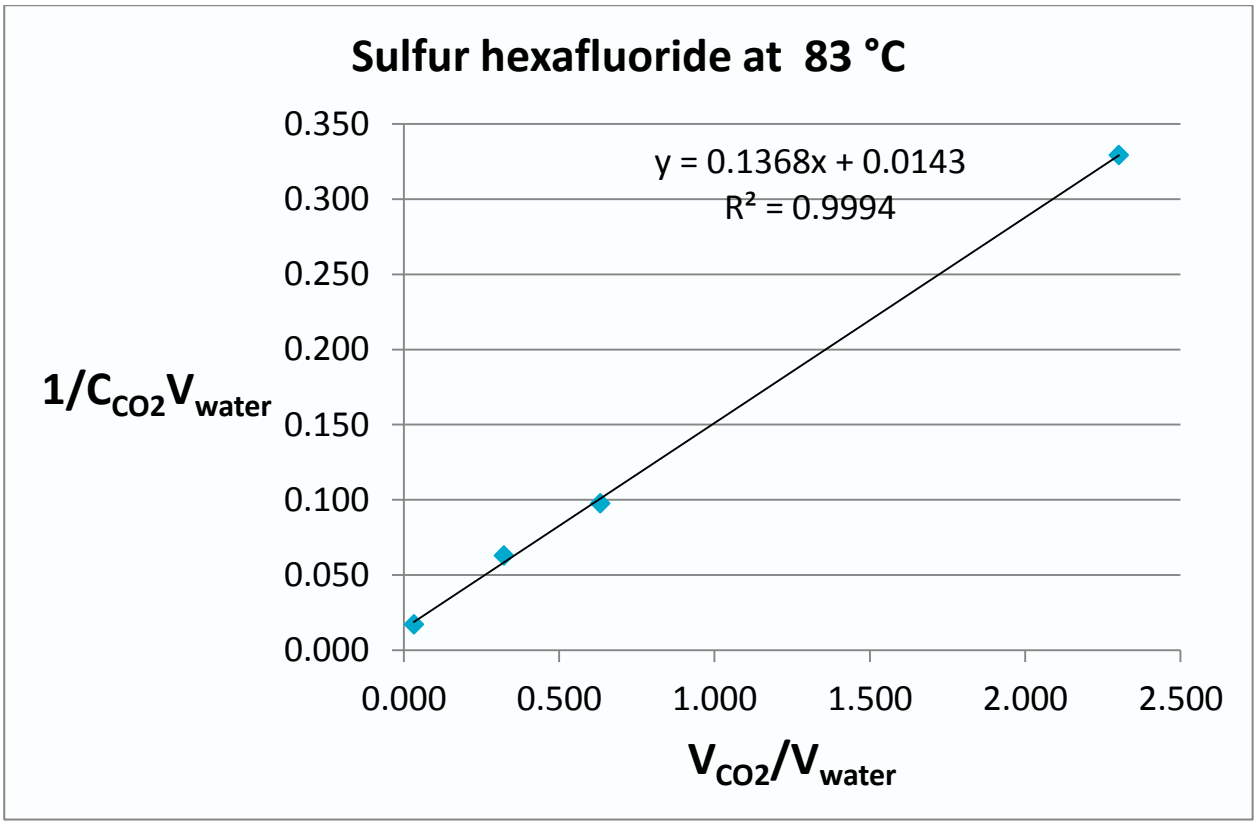

Figure 14 $1/C_{CO2}V_{water}$ vs. V_{CO2}/V_{water} plot for krypton at 59 °C

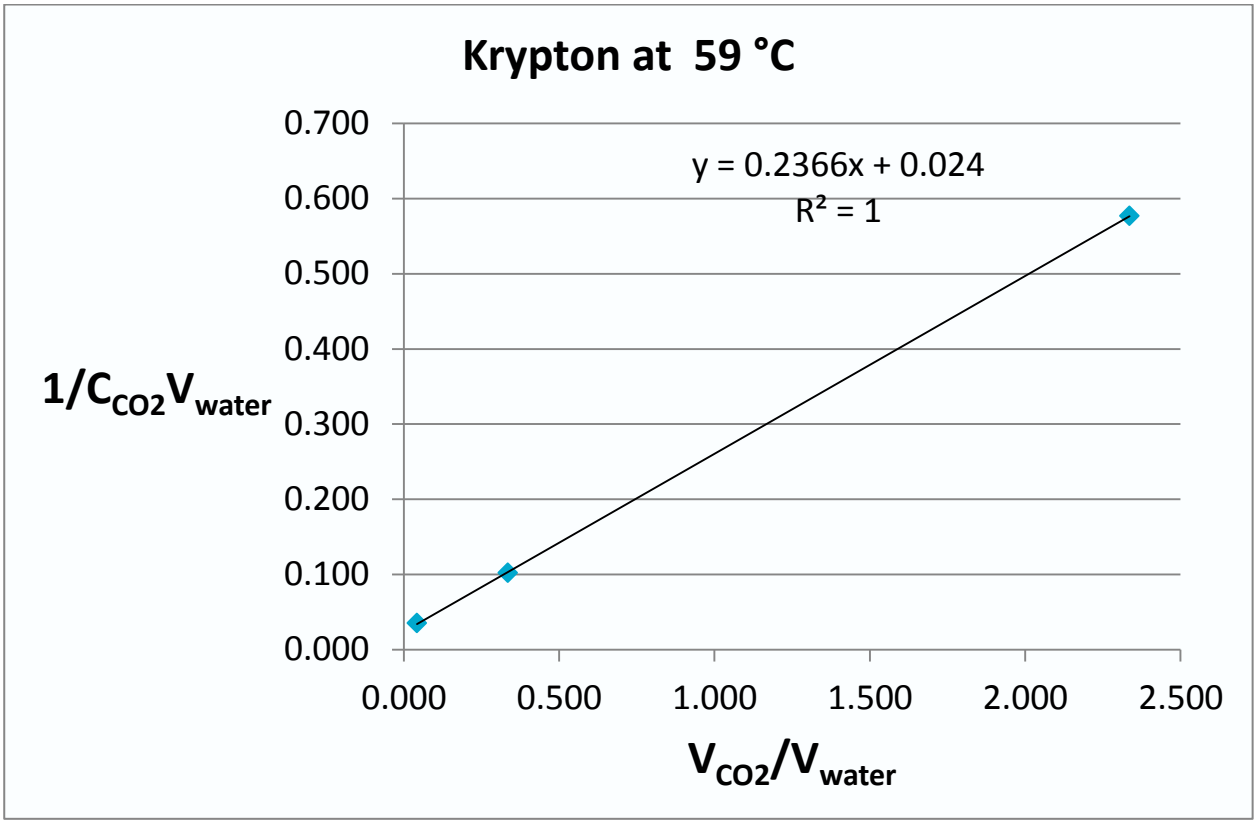

Figure 15 $1/C_{CO2}V_{water}$ vs. V_{CO2}/V_{water} plot for krypton at 83 °C

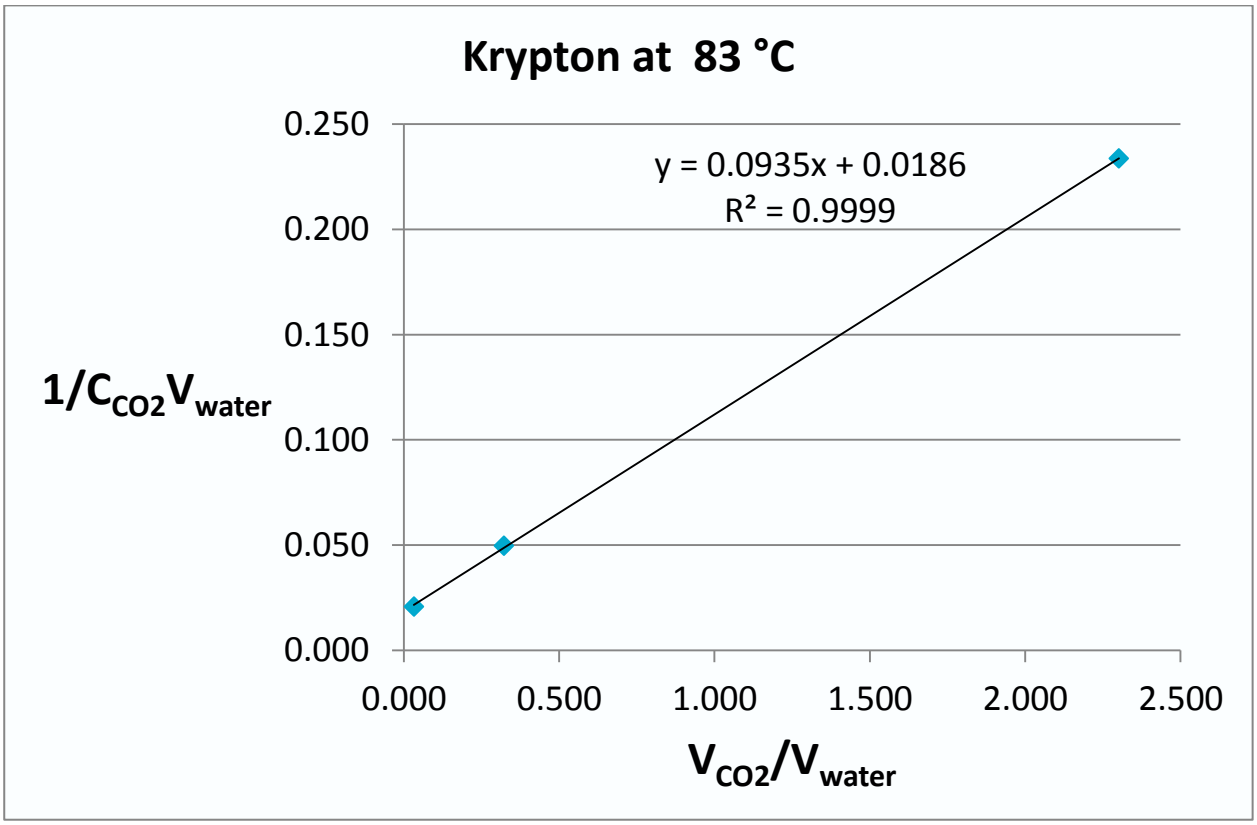

Figure 16 $1/C_{CO2}V_{water}$ vs. V_{CO2}/V_{water} plot for xenon at 59 °C

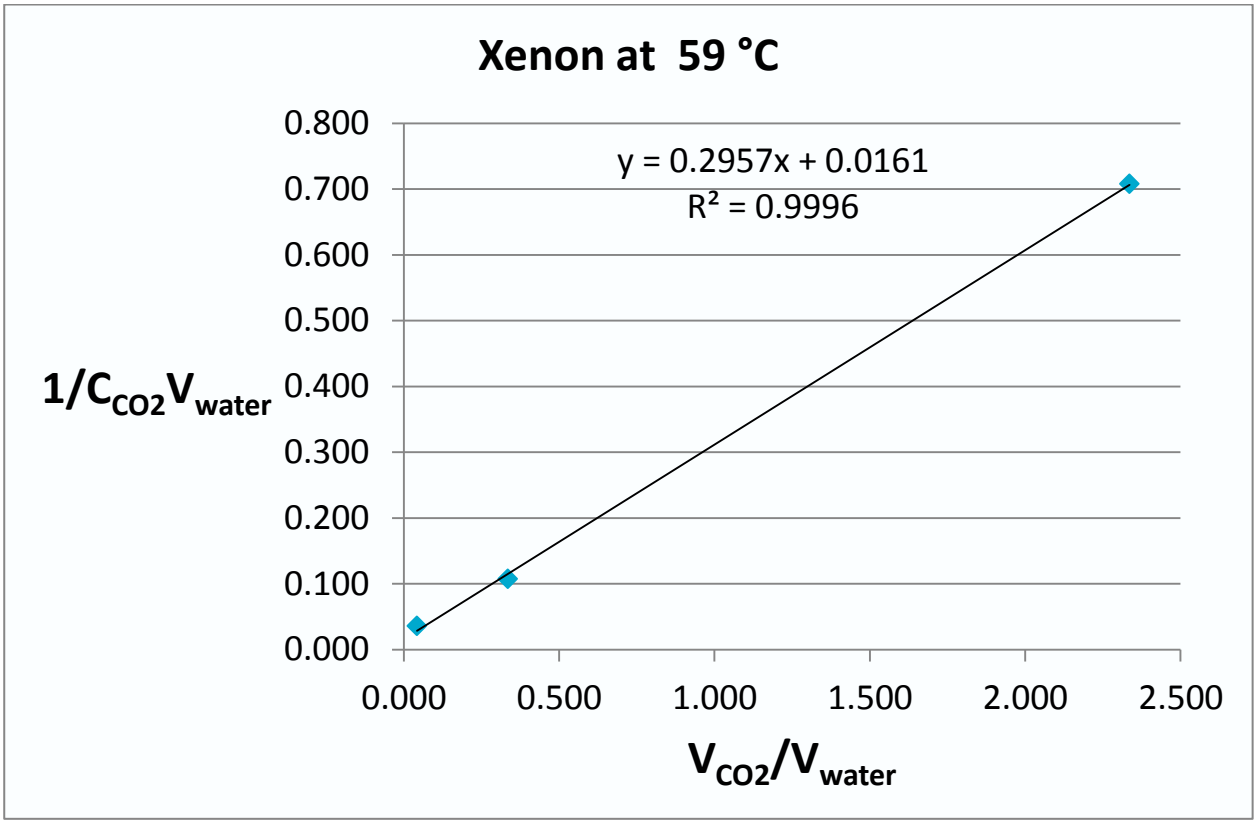

Figure 17 $1/C_{CO2}V_{water}$ vs. V_{CO2}/V_{water} plot for xenon at 83 °C

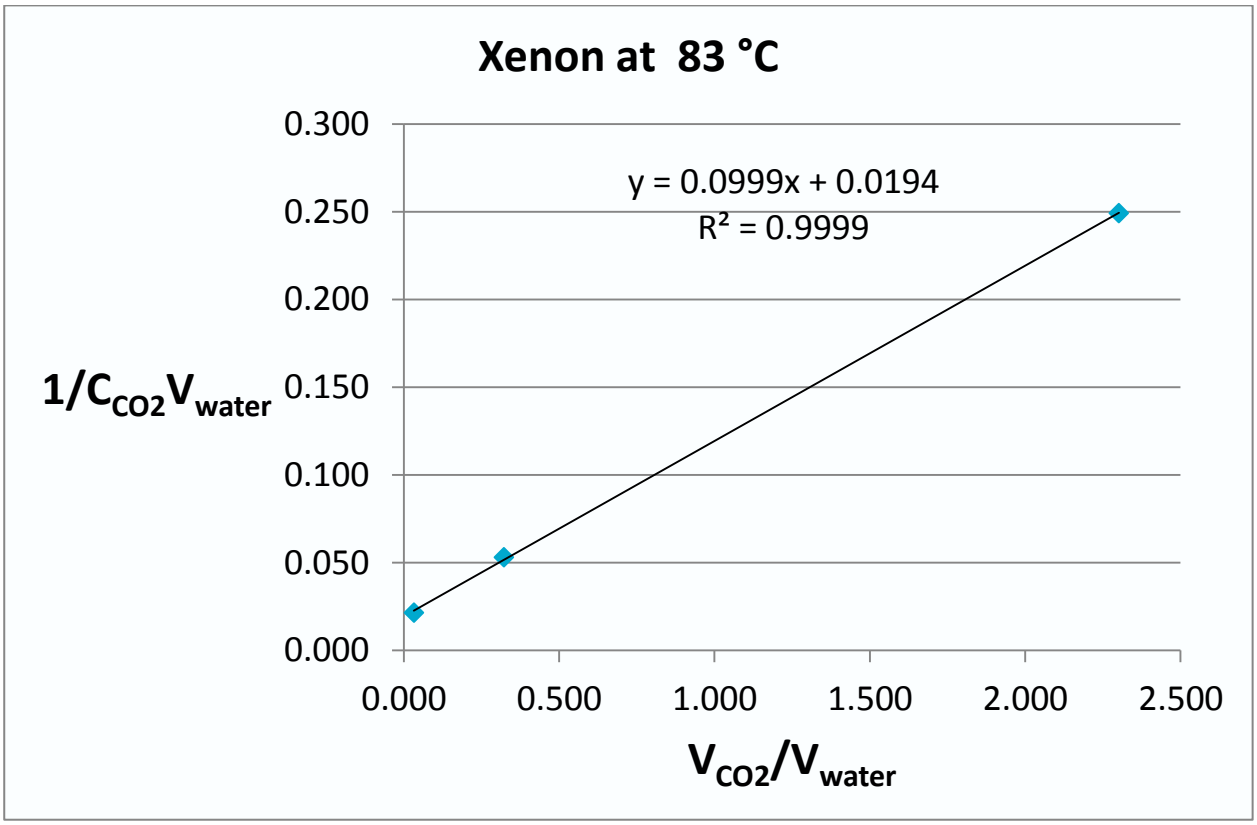

Figure 18 $1/C_{CO2}V_{water}$ vs. V_{CO2}/V_{water} plot for R134a at 59 °C

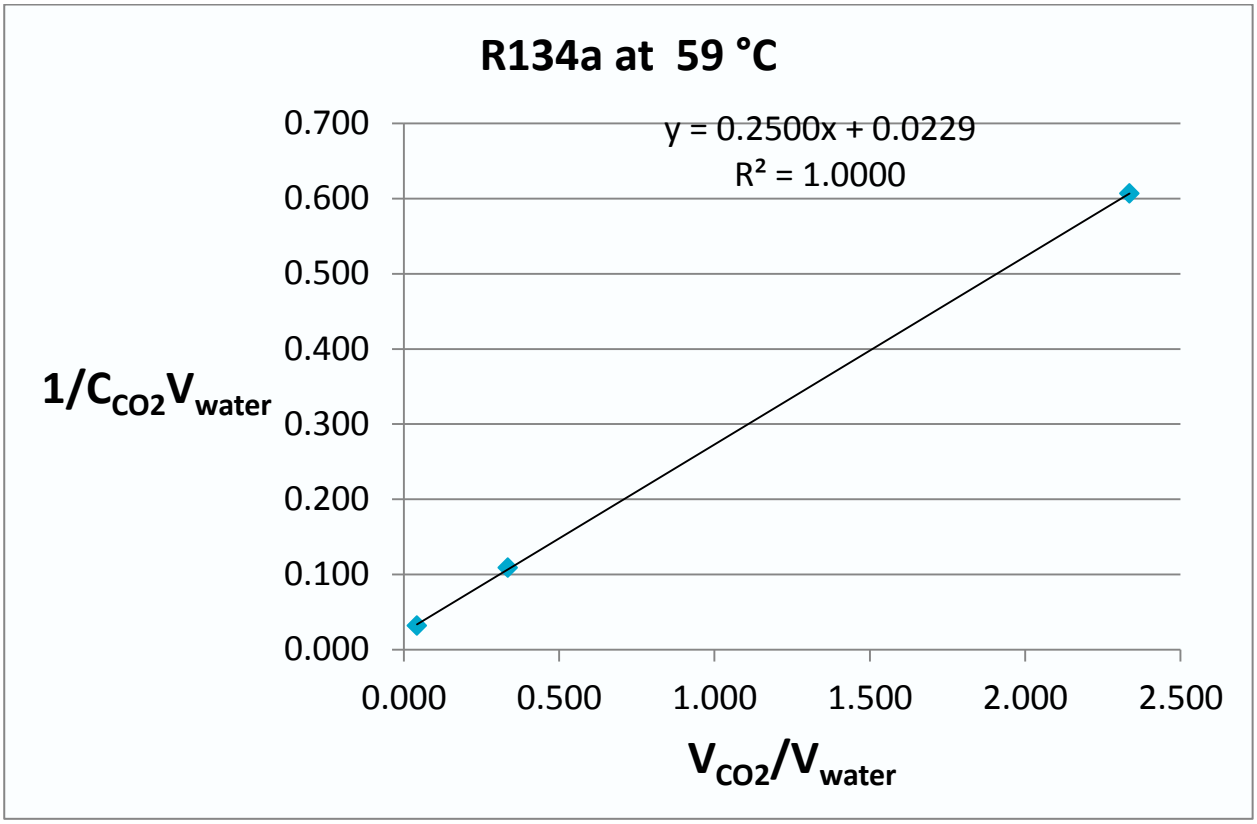

Figure 19 $1/C_{CO2}V_{water}$ vs. V_{CO2}/V_{water} plot for R134a at 83 °C

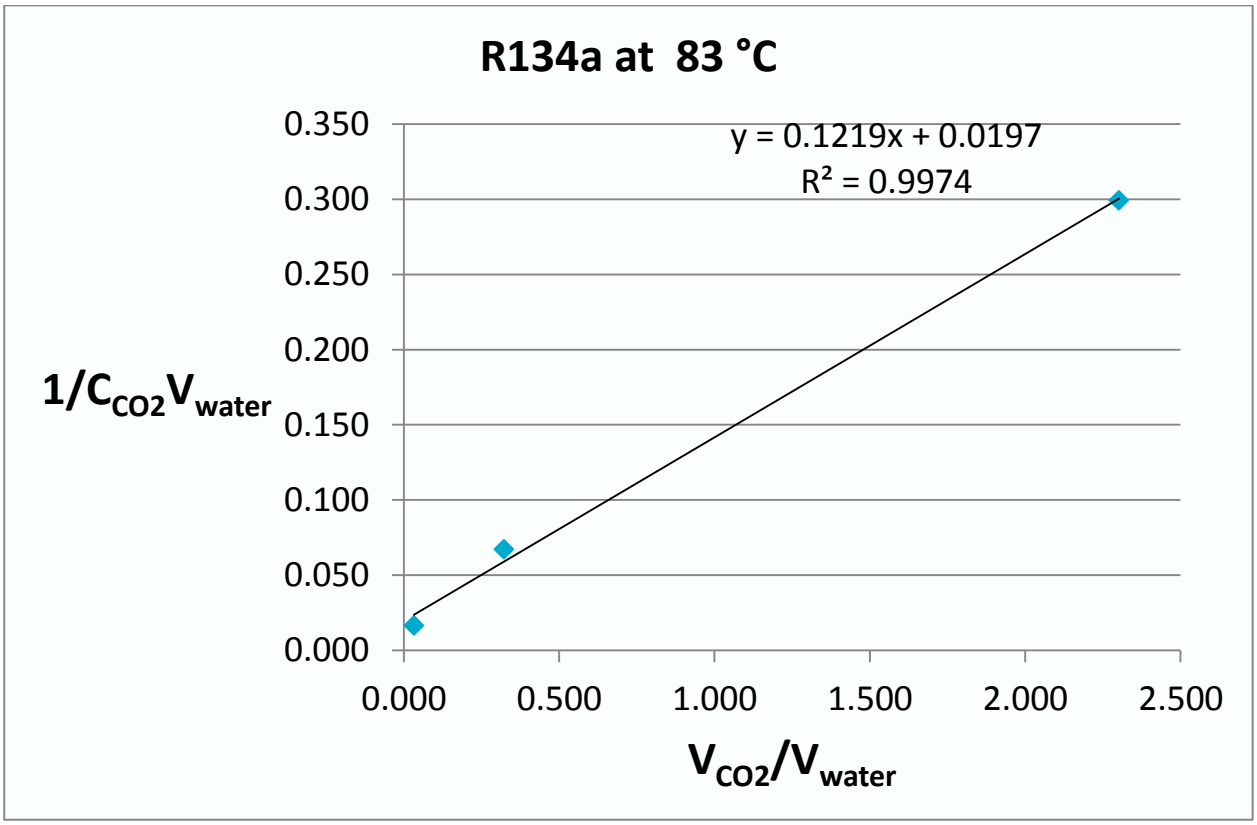

Figure 20 $1/C_{CO2}V_{water}$ vs. V_{CO2}/V_{water} plot for perdeuterated methane at 59 °C

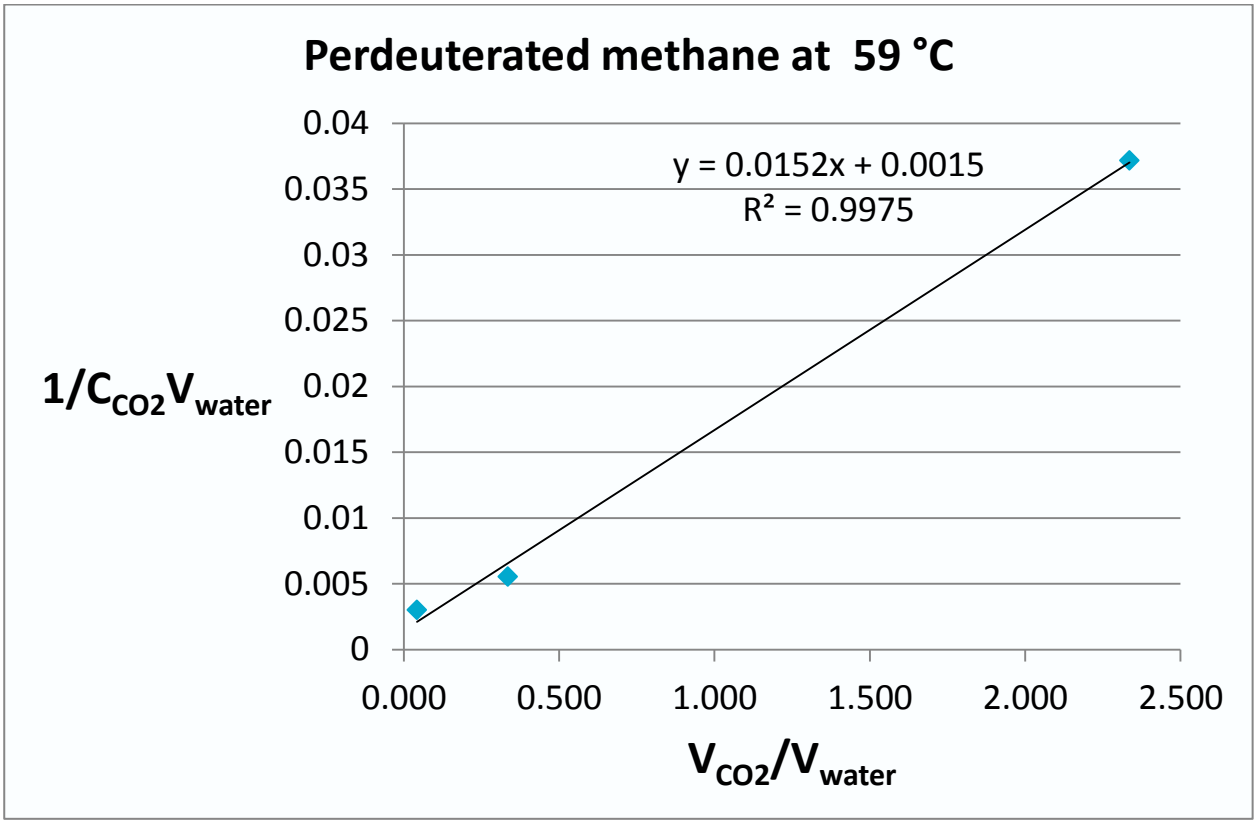

Figure 21 $1/C_{CO2}V_{water}$ vs. V_{CO2}/V_{water} plot for perdeuterated methane at 83 °C

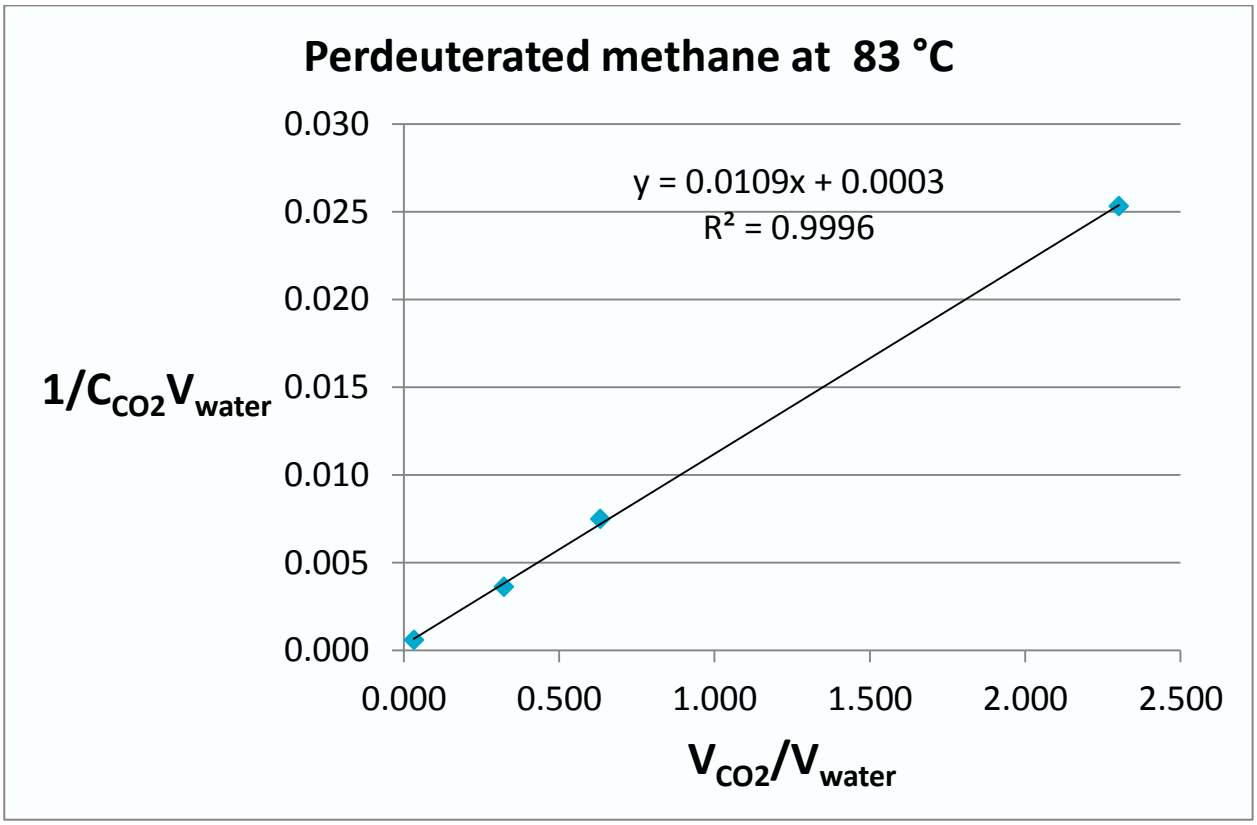

Table 8 Dimensionless (mole-basis) supercritical CO_2/water partition coefficients with associated errors, $K_{c/w}$, for inert gas tracers at 59 and 83 °C

Compound	$K_{c/w}$, 59 °C	$K_{c/w}$, 83 °C
Sulfur hexafluoride	18 ± 11	9.5 ± 3.3
Krypton	9.9 ± 0.21	5.0 ± 0.07
Xenon	18 ± 84	5.2 ± 0.13
R134a	11 ± 0.96	6.2 ± 6.5
CD_4	10 ± 53	37 ± 501

As seen in Table 8, several of the estimates have very large errors bars. Ramachandran et al. have shown that in many instances to obtain partition coefficient estimates with the method used here it is necessary to apply weighted regression. Generally, for linear regressions, weighting factors based on the inverse of the variance for the dependant variable (i.e. concentration) can be applied assuming no error in the independent variable (i.e. volume ratio). The necessary weighting factors are briefly discussed in Part II, Section 1.5 of this report. The partition coefficients using weighting coefficient is given in Table 9 below.

Table 9 Dimensionless (mole-basis) supercritical CO_2/water partition coefficients, $K_{c/w}$, for inert gas tracers at 59 and 83 °C and comparison with dimensionless (mole-basis) air/water partition coefficients, $K_{a/w}$ (derived from literature references for Henry's coefficients, Part 1)

Compound	$K_{c/w}$, 59 °C	$K_{c/w}$, 83 °C	$K_{a/w}$, 83 °C
Sulfur hexafluoride	15.1 ± 1.3	10.9 ± 1.3	1873
Krypton	9.4± 0.06	5.3 ± 0.06	156
Xenon	11.9 ± 5.0	5.6 ± 0.11	247
R134a	12.1 ± 0.40	10.8 ± 11.3	36
CD_4	5.7 ± 6.1	47 ± 37	297

Re-analysing the data using these weighting factors, there is a significant improvement in the associated errors for each partition coefficient. With the exception of CD_4, the partition coefficients decrease with increasing temperature from 59 to 83 °C. Le Chatelier's principle indicates that the partitioning process from the water phase into the supercritical CO_2 phase is exothermic for sulphur hexafluoride, krypton, xenon and R134a and endothermic for CD_4.

As can be seen by the larger errors associated with some estimates for $K_{c/w}$ above approximately 10, the method used in this series of tests for determining partition coefficients presents some practical limitations. Hypothetically, in these cases, either the y-intercept needs to be small and/or the slope needs to be large. For the partition coefficients with large errors, regression analysis shows that this is associated with errors in the determination of the y-intercepts. The reasons for these large errors are predicated in part by the range of volume ratios (V_{CO2}/V_{water}) that are used here and the amount of tracer. The regression equation suggests that reducing the amount of tracer added would lead to both a larger slope and y-intercept; however, this strategy will probably fail in that errors associated with GCMS measurements would dominate. In order to improve measurement error in this case, very low CO_2/water ratio experiments need to be conducted yielding an improvement in the error associated with the y-intercept. However,

conducting such experiments is difficult due to practicalities in sampling from the supercritical CO_2 phase when the ratio is small.

Comparison with air/water partition coefficients shows considerable differences for SF_6 and CD_4 suggesting that supercritical CO_2 is having a strong influence on their partitioning behaviour. This is most notable for CD_4 which shows a complete reversal in behaviour. For Kr, Xe and R134a, the differences are less significant; however, they are substantial enough to result in differences in the modelling and subsequent interpretations of tracer behaviour. These differences in the partition coefficient are expected to manifest themselves through changes in the results of computational simulations of chemical tracer behaviour in the subsurface. This will be the subject of the next milestone.

3 Conclusion

As part of the current project we will revisit the field tracer data from Stage 1 and Stage 2 of the Otway project (Boreham et al., 2011; Paterson et al., 2013). In the time since the initial modelling work on the stage 1 data, there has been substantial learning about tracers in the reservoir. First and foremost, accurate partition coefficients for the tracers used in the two Otway projects have recently been measured as part of the current project. Additional insight about the dispersion of tracers in the field was gained through analysis of the noble gas tracer data in the stage 2b residual trapping project. We will expand on this work with a similar analysis on the reactive tracer data, comparing several combinations of tracer curves to validate the current estimates.

Nearly four years of additional post-injection tracer data from stage 1 has also been collected at the monitoring well. Using previously developed models alongside the new partitioning and field data we will initially test the predictive capability of the existing field models. Then we will make improved dynamics models of the field to interpret the collected tracer data. It is our aim to improve general understanding of reactive and partitioning tracers with the Otway Stage 1 and 2b projects as example cases. The results of these investigations will be reported in the next and final milestone. The final milestone will also include results of experiments examining the influence of methane addition to supercritical CO_2 to mimic Buttress gas at the CO2CRC's Otway project (i.e. 20 % methane/80 % CO_2).

Part V Final Report

Reporting of year 2 activities with data generated from the high pressure/high temperature experiments and detailed interpretations documented on the experimental results acquired for the high temperature and pressure partitioning experiments between supercritical CO_2 and variable formation water chemistries; and/or methane both. Protocols and parameters for both simple partitioning pressure vessel tests and core flood experiments. The results of the validation of this partition data with current reservoir fluid models (CO2CRC Otway stage 1 site) will also be documented.

Executive Summary:

This final report summarizes the experimental work completed in the 2nd year of this project. The data acquired in the 2nd year have been combined with the data from the 1st year to achieve a robust determination on the supercritical CO_2/water partitioning data. The acquisition of new data in the last 6 months of this project combined with improved methodologies for error analysis have resulted in variations to the data provided in previous reports.

In this first section of this final report, the supercritical CO_2/water partition coefficients for the reactive ester tracer (propylene glycol diacetate, triacetin and tripropionin) are provided over the temperature range from 60 °C to 120 °C. These partition coefficients were determined by directly measuring the concentrations in both the supercritical CO_2 and water phases. For all three tracers, there is a strong temperature dependence on the partitioning behaviour. Using the van't Hoff equation, estimates for the enthalpy of the partitioning process range from -52 kJ/mole (for propylene glycol diacetate) to -83 kJ/mole (for tripropionin). Not surprisingly, this strong temperature dependence (indicated by the large enthalpy values) is expected to have a significant influence on the interpretation of single well chemical tracer tests if using these tracers to determine residual CO_2 saturation. For an accurate determination of the residual CO_2 saturation, it is therefore critical that the reservoir temperature is incorporated into the analysis of the field data.

In the second section of this report the CO_2/water and 80 % CO_2/20 % CH_4/water partition coefficients are given for krypton, xenon, sulphur hexafluoride, perdeuterated methane and R134a. Using a modification of the EPICS (or Equilibrium Partitioning in a Closed System) method, we have been able to determine these partition coefficients by only measuring the tracer concentration in the gas phase. This is advantageous as determination of dissolved concentrations in the water phase can be challenging to accomplish quantitatively. A linear regression analysis is conducted on the experimental data and the partition coefficient is derived simply as the ratio of the slope over the y-intercept. For the linear regression analysis necessary for this method, the data points have been weighted appropriately and the 95% confidence intervals have been estimated using the slope/y-intercept covariance matrix generated from the linear regression. In some instances, the experimentally determined partition coefficients have relatively small 95% confidence intervals. However, in other instances, the 95% confidence interval is quite large; this is particularly problematic for the larger partition coefficients. This is due to the nature of the experiment where the y-intercept from the regression analysis is very near the zero point. For larger partition coefficients where the y-intercept is small, being in the denominator of the ratio, small variations in the y-intercept impact the error for this method significantly. Careful attempts have been made to reduce this uncertainty by obtaining duplicate samples and by using a wide

range of volume ratios. This data set has allowed us to constrain the possible values for the partition coefficients and this has resulted in the conclusion that the partition coefficients determined here are generally very different than related air/water partition coefficients.

Using a number of assumptions, analytical solutions for injected tracer behaviour into a homogeneous reservoir can be obtained. This approximation allows for a qualitative comparison between the behaviour of tracers with differing partition coefficients to be ascertained. This analysis shows that there is a significant impact on the predicted tracer behaviour with differing partition coefficients providing more confidence in the comparisons with field data. Following this analysis and the conclusions derived from it, computational simulations using TOUGH2 have been conducted on the Otway Stage 1 data. Evidence suggests that:

- The air/water partition coefficients are generally much higher than their corresponding supercritical CO_2/water partition coefficients.
- Both analytical solutions and the TOUGH2 simulations show that for the air/water partition coefficients there is an earlier and simultaneous arrival of tracer; whereas, supercritical CO_2/water partition coefficients result in a later arrival of tracer with some chromatographic separation of the tracers.
- The initial breakthrough concentration is expected to be much higher with the air/water partition coefficients relative to the CO_2/water partition coefficients.

With either set of partition coefficients, the fit is not perfect and the discrepancies with each fit could be explained possibly by other phenomena (e.g. sorption, low sampling temporal resolution). Given these circumstances, it is difficult to determine which set of partition coefficients provides a better fit to the field date from Otway.

Based on the reservoir simulations conducted as a part of this study we can conclude that for unbounded reservoirs (i.e. those without a capping structure) the impact of the new partition coefficients on the simulated transport of the inert gas tracer in the reservoir is minor and potentially significant. We believe for an unbounded reservoir scenario that these differences could possibly be detected through field trials and the choice of partition coefficients would affect the outcomes from computational simulations. However, for the bounded reservoirs studied here, the effect on the behaviour is negligible and it is highly unlikely that there would be any differences in the outcomes from computational simulations of field trials.

1 Reactive tracer partition coefficients

1.1 Experimental results

In Table 10, the revised partition coefficients based on the complete data set derived from this project is given for the reactive ester tracers.

Table 10 Experimentally determined mole fraction basis partition coefficients and associated standard error for the reactive tracers at temperatures ranging from 62 to 110 °C

Chemical Name	Temp (°C)	$K^x_{c/w}$	$U(K^x_{c/w})$
Propylene glycol diacetate	62	54.5	0.05
Propylene glycol diacetate	70	18.1	0.10
Propylene glycol diacetate	90	8.5	0.17
Propylene glycol diacetate	100	5.8	0.13
Propylene glycol diacetate	110	3.3	0.18
Propylene glycol diacetate	120	2.9	0.08
Triacetin	62	27.7	0.10
Triacetin	70	8.2	0.07
Triacetin	85	3.4	0.03
Triacetin	110	1.1	0.03
Triacetin	120	0.7	0.05
Tripropionin	62	313	0.09
Tripropionin	70	121	0.10
Tripropionin	85	29.1	0.15
Tripropionin	90	9.3	0.13
Tripropionin	110	7.2	0.17

1.2 Interpretation of the results

For the single well tracer test using reactive ester tracer, the method of moments provides a simple formulation for estimating the residual saturation by knowing the relevant partition coefficients, K_p *and* K_h, and the elution times, t_p and t_h, for both the parent ester tracer and the hydrolysis daughter tracers, respectively. The relevant mathematical derivation to determine residual saturation is provided below.

During water production to recover fluids from the reservoir interval, the parent tracer and its hydrolysis product will elute differentially and by characterizing these differences the residual CO_2

saturation can be determined. The method of moments can be used to explain these chromatographic processes occurring during water production for both the parent tracer and its hydrolysis product(s) and relies on knowing only the relative retention times along with the partition coefficients. The method is based solely on the relative velocities of each of the tracers and as such can provide a rough estimate of the residual $C0_2$ saturation.

During initial injection of the ester tracer into the well under investigation, a plug of water containing the tracer is pushed a distance *L* radially away from the injection wellbore. After a "shut-in" or "soak" period (the length of time is dictated by the kinetics of the hydrolysis reaction) where the tracers are held in place, hydrolysis product are generated. The velocity of the tracer *v* during tracer/water production is given as the time weighted average

$$v = fv_w + (1-f)v_C$$

where *f* is the fraction of time the tracer spends in the water phase and v_w and v_c are the velocities of the water and carbon dioxide phase respectively. As the carbon dioxide is residually trapped, v_c is assumed to be zero and the time weighted velocities are simply

$$v = fv_w.$$

After the hydrolysis reaction both the parent tracer and its hydrolysis products are collocated after the hydrolysis reaction (i.e. the tracers do not move during the "shut-in" period) and as such the distance each travels will be the same during tracer/water production. Therefore the retention time for the tracer is

$$t = \frac{L}{fv_w}.$$

S_c and S_w are the volume fractions of carbon dioxide and water respectively relative to total pore volume and $S_c + S_w = 1$. The number of molecules of each tracer in the water phase (n_w) and supercritical carbon dioxide (n_c) in a volume *dV* is then

$$n_w = c_w S_w dV \text{ and } n_c = c_c S_c dV,$$

where c_w and c_c are the concentrations of compound *i* in water and supercritical carbon dioxide, respectively. The partition coefficient for each tracer is defined as

$$K = \frac{c_c}{c_w} \text{ (based on concentration).}$$

The retardation factor (defined as the ratio of the amount of compound in the supercritical carbon dioxide and water or n_w/n_c) is

$$r = \frac{KS_c}{1-S_c}.$$

Probability theory then suggests that

$$\frac{1-f}{f} = r \text{ or } f = \frac{1}{1+r}.$$

By comparing the relative behavior of both tracers (denoted by the subscripts *p* and *h* for the parent tracer and its hydrolysis product, respectively), the following expression is obtained:

$$\frac{r_p}{K_p} = \frac{r_h}{K_h} = \frac{S_c}{1-S_c}.$$

It follows that

$$L = v_w t_p f_p = v_w t_h f_h.$$

Rearranging this expression, the following expressions are obtained:

$$\frac{t_p}{t_h} = \frac{f_h}{f_p} = \frac{1+r_p}{1+r_h} = \frac{1+\frac{K_p S_c}{1-S_c}}{1+\frac{K_h S_c}{1-S_c}}$$

The residual saturation is calculated by solving the above equation for S_c:

$$S_C = \frac{\frac{t_p}{t_h}-1}{\frac{t_p}{t_h}(1-K_h)+K_p-1}.$$

Figure 22 is made by combining this final equation for S_c with the van't Hoff temperature dependence for the partition coefficients (a hypothetical scenario is detailed in the caption of Figure 22) showing the relationship between reservoir temperature and the estimate residual saturation. It is clear that there is a significant impact on the estimate of residual saturation with reservoir temperature. Thus any uncertainty in the reservoir temperature (possibly due to cooling during CO_2 or CO_2/water injection) could have an impact on the interpretation of the tracer results.

Figure 22 Plot of the estimated CO_2 residual saturation vs. reservoir temperature for t_p/t_h ratios of 1.5, 2, 3, 4 and 5 and partition coefficients, $K_{c/w}$, at 62 °C of 5 and 0.2 for the parent tracer (ΔH ~ 60 kJ/mole) and for the hydrolysis product (ΔH ~ 0 kJ/mole), respectively

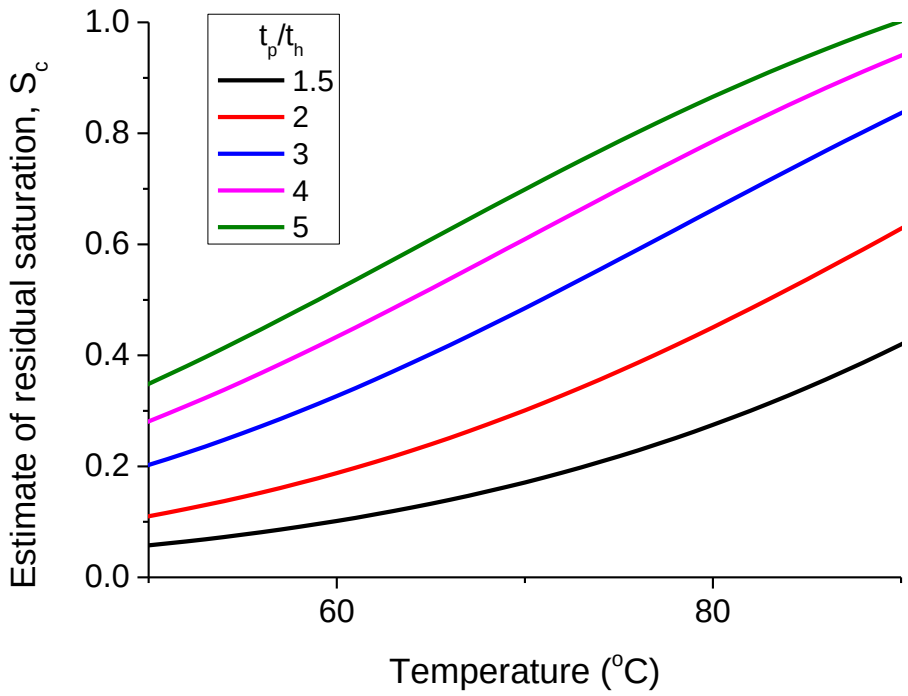

2 Inert gas partition coefficients

In this section, the revised partition coefficients based on the complete data set for this project along with necessary fitting parameters are given for the inert gas tracers. In the next section, a detailed analysis of the impact that these results have on computational simulations of tracer behaviour for Otway Stage 1 is given.

2.1 Partition coefficients between CO_2 and water

Table 11 Inert gas tracer partition coefficients between pure CO_2 and water

Temp. (°C)	Tracer	Number of Volume Ratios	Number of Data Points	Slope	Y-intercept	$K_{c/w}$ conc. basis	95% confidence interval	R^2	$K^x_{c/w}$ Mole fraction basis	Inverse Henry's Coefficient for TOUGH2 (Pa^{-1})
59	Kr	4	6	0.177	0.039	4.50	3.42	0.987	18.86	1.46E-09
59	Xe	4	6	0.192	0.040	4.87	3.03	0.993	20.41	1.35E-09
59	sf6	4	6	0.218	0.024	8.93	19.00	0.973	37.41	7.35E-10
59	CD4	4	6	0.012	0.003	3.72	3.27	0.986	15.60	1.76E-09
59	R134a	4	6	0.192	0.063	3.04	3.10	0.975	12.76	2.15E-09
83	Kr	5	10	0.089	0.017	5.12	0.53	1.000	23.40	1.19E-09
83	Xe	5	10	0.102	0.012	8.58	4.23	0.998	39.21	7.13E-10
83	sf6	5	10	0.096	0.025	3.79	2.04	0.992	17.34	1.61E-09
83	CD4	4	8	0.011	2.26E-04	47.01	33.20	1.000	214.76	1.30E-10
83	R134a	4	8	0.129	0.015	8.67	7.04	0.995	39.60	7.06E-10

2.2 Partition coefficient between 80% CO_2 / 20% CH_4 and water

Table 12 Inert gas tracer partition coefficients between 80% CO_2/20% CH_4 and water

Temp. (°C)	Tracer	Number of Volume Ratios	Number of Data Points	Slope	Y-intercept	$K_{c/w}$ conc. basis	95% confidence interval	R^2	$K^x_{c/w}$ Mole fraction basis	Inverse Henry's Coefficient for TOUGH2 (Pa^{-1})
59	Kr	4	8	6.04E-05	4.29E-06	14.08	15.70	0.995	104.43	4.66E-10
59	Xe	4	8	6.29E-05	2.69E-06	23.42	110.00	0.977	173.66	2.80E-10
59	sf6	3	6	6.22E-05	7.07E-06	8.80	7.21	0.997	65.23	7.46E-10
59	CD4	4	8	1.24E-05	9.07E-07	13.72	16.20	0.995	101.71	4.78E-10
59	R134a	4	8	6.96E-05	5.74E-06	12.11	19.70	0.987	89.82	5.41E-10
83	Kr	4	8	5.90E-05	6.79E-06	8.69	6.38	0.996	58.87	7.04E-10
83	Xe	4	8	8.73E-05	4.55E-06	19.21	49.90	0.986	130.16	3.18E-10
83	sf6	4	8	1.13E-04	1.36E-05	8.32	18.90	0.951	56.35	7.36E-10
83	CD4	4	8	1.04E-05	1.87E-06	5.55	10.30	0.951	37.61	1.10E-09
83	R134a	5	10	8.44E-05	1.00E-05	8.42	9.42	0.988	57.09	7.26E-10

3 The impact of inert gas tracer partition coefficients on flow in porous media

The purpose of this study is to establish general observations on the impact of differing chemical tracer partition coefficient values on the arrival time and shape of tracer breakthrough profiles at a monitoring well. Initially very simple one-dimensional analytical models are considered, and then two-dimensional simulations of an idealised reservoir are simulated. Using simplified models such as these initially makes it possible to discern changes in the predicted tracer behaviour caused by using new partition coefficient values in the absence of changes that are the result of other physical mechanisms in the model (e.g. phase partitioning of the fluids, heterogeneity in the geology and reservoir filling mechanism).

3.1 Analytical modeling

Chromatographic separation theory can be used to analyse how changes in partition coefficients between the gas and water phases impact on tracer behaviour in a reservoir based only on the composition of the injection and reservoir fluids. Analytical solutions can be rigorously developed subject to a number of conditions (Orr, 2007). In particular, it is assumed that displacements are one-dimensional and dispersion-free, the injection gas composition is constant over time with continuous injection of tracer, the initial reservoir composition is homogeneous and the partition coefficients are independent of the overall composition of the system. Orr et al. details a more complete list of assumptions necessary for using this theory (known as the method of characteristics) as well as a detailed discussion of how to quantitatively construct displacements for four-chemical component systems that partition between two fluid phases in the reservoir.

It is convenient to consider partition coefficients for the various chemical components in a system as K-values based on the mole fraction of each component in each phase: $K_i = y_i/x_i$, where y_i is the mole-fraction of component *i* in the gas (or supercritical) phase and x_i is the mole-fraction of component *i* in the aqueous phase. The 10th column of Tables 12 and 13 show the partition coefficients for all the tracers for the laboratory results from the present study. The last column in Table 9 in Part IV of this report shows the Henry's Law coefficients from air/water data converted into mole-based partition coefficients. To build analytical solutions for the tracer behaviour mole basis K-values are also necessary for H_2O, CH_4 and CO_2 which have values ranging between 0.007-0.009, 616-831 and 40-54, respectively.

The key factor in assessing the behaviour of tracers in the reservoir, and consequently the tracer production profiles in a monitoring well, is the relative magnitudes of the K-values for the various chemical components. Each one-dimensional analytical displacement will traverse three key tie-lines: the injection gas tie line, the initial reservoir tie line, and the cross-over tie line that connects them. A tie line is defined as the line in composition space that connects the equilibrium liquid and gas phase compositions for a mixture of components that forms two phases at constant reservoir temperature and pressure (Orr, 2007). The injection and initial tie lines are fully determined by the boundary conditions and only the cross-over tie line must be found. The relative differences in the K-values will determine the location of the cross-over tie

line. It is sufficient for the present purposes to sketch the behaviour of the analytical solutions qualitatively to show the impact of partition coefficients on expected tracer production peaks.

Two initial conditions will be considered analytically: (1) injection into an aquifer and (2) injection into a gas field with a gas cap of only CH_4. For each initial reservoir condition, two injection mixtures are considered: (1) pure CO_2 and (2) a mixture of 80% CO_2 and 20% CH_4.

As can be seen in Tables 9, 12 and 13, the ordering of the K-values for tracers, CO_2 and CH_4 is quite different for air/water partition coefficients reported in the literature and the supercritical CO_2/water partition coefficients determined as part of this project. In particular there are four possible scenarios for K-value ordering at 83°C:

- Case 1: $K_{CH4}>K_{CO2}>K_{Tr}$, for Tr = $R134a_{aw}$, $R134a_{pure}$, Kr_{pure}, Xe_{pure}, $CD_{4,80/20}$ and $SF_{6,pure}$
- Case 2: $K_{CH4}>K_{Tr}>K_{CO2}$, for Tr = $CD_{4,aw}$, Xe_{aw}, Kr_{aw} $CD_{4,pure}$ and $Xe_{80/20}$
- Case 3: $K_{Tr}>K_{CH4}>K_{CO2}$, for Tr = $SF_{6,aw}$
- Case 4: $K_{CH4}>K_{CO2}\cong K_{Tr}$, for Tr = $R134a_{80/20}$, $Kr_{80/20}$ and $SF_{6,80/20}$.

Where the subscript *aw* denotes the air/water partition coefficients, *pure* denotes the laboratory data for pure CO_2/water coefficients and *80/20* denotes the laboratory determined coefficients for mixed CO_2/CH_4 and water. These four possibilities result in three distinct types of displacement. For case 4, where the tracer partition coefficient is indistinguishable from the CO_2 coefficient, the displacement may appear similar to case 1 or case 2. It is possible to qualitatively demonstrate all four possible displacement types with just four examples.

3.1.1 CASE 1: $K_{CH4}>K_{CO2}>K_{TR}$

Given the generally low solubility of inert gas tracers in water, it is somewhat unexpected that the behaviour predicted for Kr_{pure}, Xe_{pure}, $CD_{4,80/20}$ and $SF_{6,pure}$ would actually be observed. In this case the partitioning of gas tracer into the water is more favourable than supercritical CO_2 partitioning into water (see Tables 12 and 13). Unlike the supercritical CO_2/water partition coefficients determined here, the Henry's law coefficients in Table 9 in Part IV of this report show that for the gas/water equilibrium all of the inert gas tracers examined here would partition much more strongly into the gas phase relative to water. $R134a_{aw}$ and $R134a_{pure}$ also partition into the water phase more preferentially than the CO_2.

Figure 23 shows the results of CO_2 injection into a depleted reservoir at residual CH_4 saturation for case 1, $K_{CH4}>K_{CO2}>K_{Tr}$. This case includes all the supercritical CO_2/water partition coefficients measured here and the air/water tracer partition coefficient for R134a. The key tie lines in the displacement increase in length from the injection tie line to the initial tie line, so this is a vaporising gas drive (Orr, 2007).

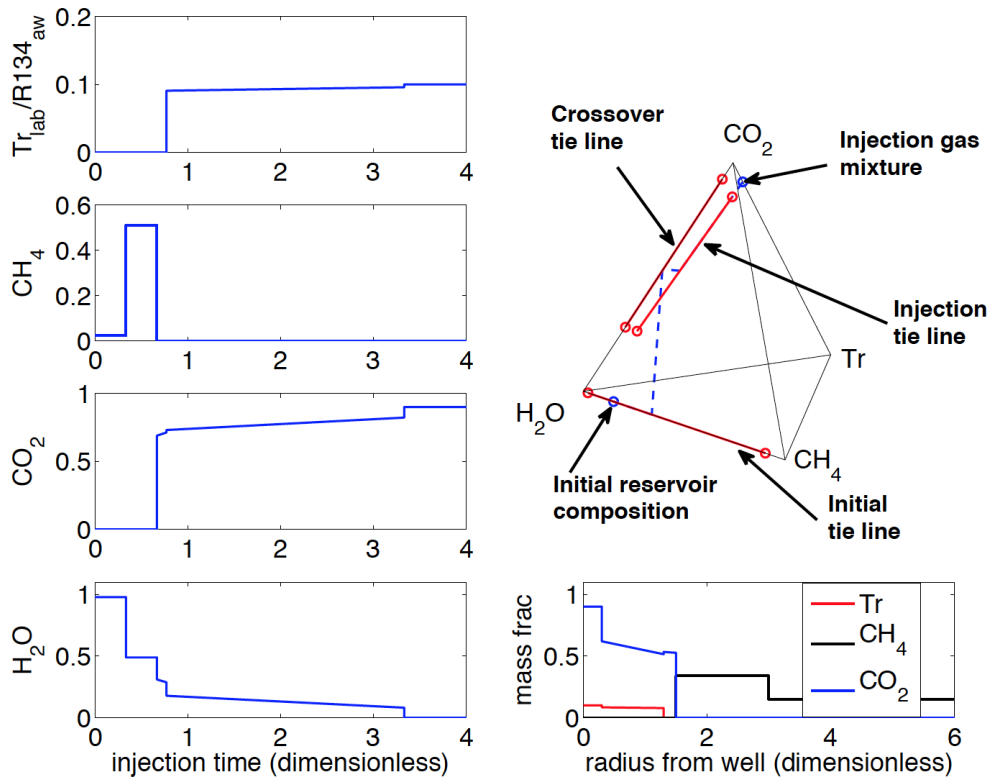

Figure 23: Left: Component production curves for case 1, $K_{CH4}>K_{CO2}>K_{Tr}$ and pure CO_2 into a depleted gas reservoir originally containing residual gas everywhere. From the top: $R134a_{aw}$, Kr_{pure}, Xe_{pure}, $CD_{4,80/20}$ or $SF_{6,pure}$ production with any of the laboratory partition coefficients, CH_4 production, CO_2 production, H_2O production. Right side from the top: composition path in quaternary space, profile of chemical components in the reservoir.

With CO_2/tracer injection, the residual CH_4 initially present in the reservoir is mobilised and moves away from the injection well ahead of the injected gases. CO_2 has a higher K-value than the injected tracer and so CO_2 moves into the reservoir ahead of the tracer. As can be seen on the left side of Figure 23, at a monitoring well the mobilised CH_4 will be observed first, followed by supercritical CO_2 and shortly thereafter the tracer will be produced. Once the tracers reach the observation well, the concentration is relatively constant in the analytical solution which presumes continuous tracer injection. In the injection scenario used at Otway where tracer was injected as a pulse, there would be a subsequent decline in the tracer concentration at the observation well.

If no residual CH_4 was present in the reservoir initially, the leading CH_4 bank would obviously be absent from the displacement, but the relative arrival times of the CO_2 and tracers would not change. Generally, with larger tracer partition coefficient K-values, there is a shorter period of time between CO_2 arrival and tracer arrival at the monitoring well.

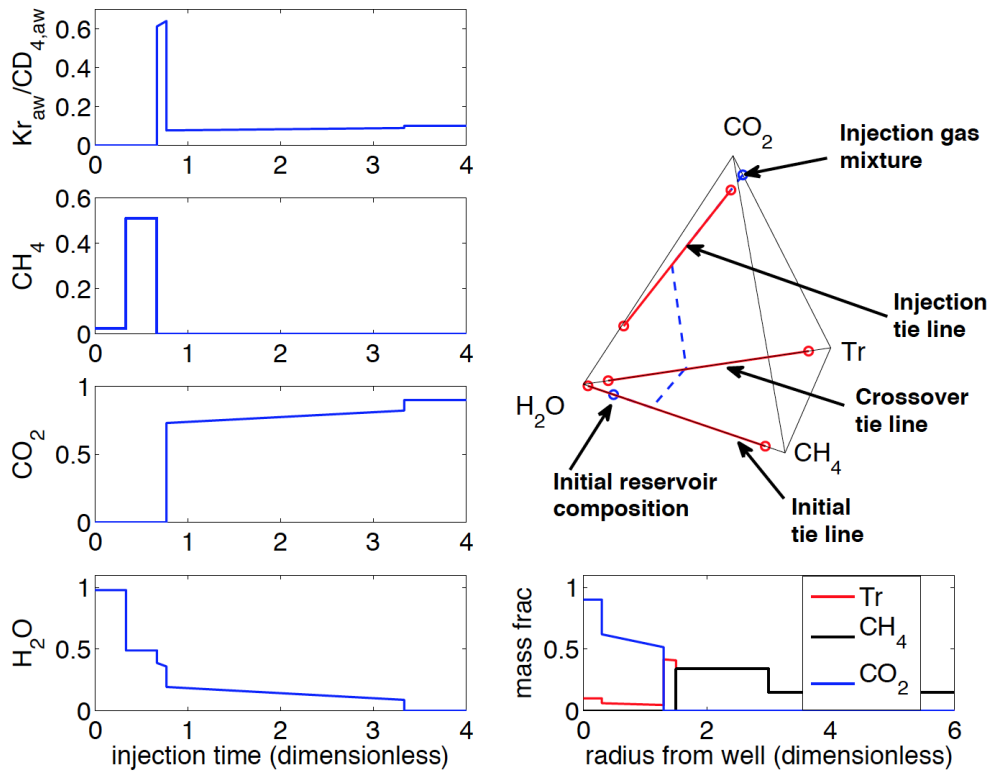

Figure 24 Component production curves for case 2, $K_{CH4}>K_{Tr}>K_{CO2}$ and pure CO_2 into a depleted gas reservoir originally containing residual gas everywhere. Left side from the top: Xe_{aw} Kr_{aw}, Xe_{aw}, $CD_{4,aw}$, $Xe_{80/20}$ or $CD_{4,pure}$ production, CH_4 production, CO_2 production, H_2O production. Right side from the top: composition path in quaternary space, profile of chemical components in the reservoir.

3.1.2 CASE 2: $K_{CH4}>K_{TR}>K_{CO2}$

In this case CO_2 is injected into a depleted gas reservoir at CH_4 residual saturation where $K_{CH4}>K_{Tr}>K_{CO2}$. The results for this scenario are summarized in Figure 24. This case applies to $Xe_{80/20}$, $CD_{4,pure}$, $CD_{4,aw}$, Xe_{aw} and Kr_{aw}. The key tie lines in the displacement increase in length from the injection tie line to the initial tie line implying a vaporising gas drive as well (Orr, 2007). Once again, tracer is injected continuously as a necessary assumption to obtain an analytical solution.

The methane bank is identical to the previous case. In this case, the tracer is the more volatile injected component, and so it forms a bank and moves into the reservoir faster than the CO_2. The resulting tracer bank has a concentration that is much higher than the initial injected concentration, but it also has a very narrow width in the reservoir, due to the small concentration of tracer injected. As a consequence, monitoring at an observation well would show a short bank of tracer that is much higher than the injection concentration before the arrival of CO_2, followed by a decline in tracer concentration to slightly below the injected concentration at CO_2 breakthrough, as can be seen in Figure 24.

3.1.3 CASE 3: $K_{TR}>K_{CH4}>K_{CO2}$

Case 3 where $K_{Tr}>K_{CH4}>K_{CO2}$ applies to $SF_{6,aw}$ and represents a physically different type of displacement because the cross-over tie line is the longest. This is a mixed condensing/vaporising displacement (Orr, 2007). The profiles of the components in the

reservoir (not shown) are extremely similar to case 2, summarized in Figure 24, with a slightly lower and wider tracer bank. In this case a high spike in tracer concentration would be observed at the monitoring well just before the arrival of CO_2.

3.1.4 CASE 4: $K_{CH4}>K_{CO2}\cong K_{TR}$

The tracers in case 4 are $R134a_{80/20}$, $Kr_{80/20}$ and $SF_{6,80/20}$. The tracer partition coefficients are a single value based on the experimental data, while the CO_2 coefficient is calculated from an equation of state and changes with overall composition, temperature and pressure. For the simulated displacements in the following section K_{CO2} is in the range 22-44.

In the reservoir the CO_2 partition coefficient may be larger or smaller than the measured partition coefficient for these tracers. This means that the tracer production curves could follow the pattern of case 1 with a low-concentration tracer bank arriving after the CO_2 or the pattern of case 2 with a high-concentration tracer bank arriving before the CO_2. It is also possible to have a switch between case 1 and case 2 mid-displacement, which would likely result in no discernible difference between tracer and CO_2 arrival times.

3.1.5 80% CO_2, 20% CH_4 INJECTION

The same analysis can be repeated for the mixed CO_2 and CH_4 injection, with similar results. The solution is somewhat more complex because CH_4 is present in both the initial reservoir and injected fluid compositions, so the crossover tie-line now contains CH_4, H_2O and tracer. However the qualitative results with respect to the formation of a leading CH_4 bank and CO_2 trailing behind are identical. For cases 2 and 3, the tracers will appear as a narrow bank with high tracer concentration between the two gas banks; while for case 1, the tracer will appear at low concentration sometime after CO_2 arrival

3.1.6 CONCLUSIONS FROM ANALYTICAL MODELLING

Based on the analytical modelling, there is a fundamental shift in the relative arrival time of the injected SF_6, and Kr tracers, and there may be a shift for Xe and CD_4 tracers when the partition coefficients are changed from air/water coefficients in the literature to the CO_2/water partition coefficients measured as a part of the present work.

- Based on the supercritical CO_2/water partition coefficients, $SF_{6,pure}$, Xe_{pure}, Kr_{pure} and $CD_{4,80/20}$ are expected to arrive at a monitoring well after the mobilised CH_4 is detected and shortly after breakthrough of the injected CO_2. Tracer concentration will be near the injected concentration value.
- For the air/water partition coefficients, $SF_{6,aw}$, Xe_{aw}, Kr_{aw} and $CD_{4,aw}$ are expected to arrive prior to the injected CO_2 at a concentration that is substantially higher than the injected concentration. At CO_2 breakthrough, tracer concentration will decline sharply to a value slightly lower than the injected concentration. $CD_{4,pure}$ and $Xe_{80/20}$ have a very similar behaviour trend.
- For R134a, the ordering of the K-values is the same for the air/water and laboratory partition coefficients, so in both cases the tracer is expected to appear at a production well at near-injection concentration, just after CO_2 breakthrough.
- For $Kr_{80/20}$, $R134a_{80/20}$ and $SF_{6,80/20}$ the partition coefficient for the tracer is in the range of the variable CO_2 partition coefficient, so it is unclear whether there will be separation between the CO_2 and tracer at a production well.

Clearly a significant level of detail has been left out of this qualitative discussion. However, at a monitoring well where the tracers are flowing past without obstruction, there should be a measurable difference between a tracer that has a high peak in concentration that arrives prior to CO_2 and a tracer with a low concentration that arrives shortly after CO_2. This assumes that mixing in the reservoir due to dispersion or heterogeneity of the formation is not too severe. Moreover, if several tracers are injected simultaneously chromatographic separation from highest to lowest partition coefficient should be observed at monitoring wells, especially if the sampling program has sufficient temporal resolution to capture this information.

3.2 Simplified two-dimensional simulations

The field geometry is chosen to be similar to the Otway Stage 1 project, as it is likely that in field CCS projects injection and monitoring well pairs will be installed in a similar orientation to this test site. For Otway Stage 1, the monitoring well is 300 *m* up-dip from the injection well and near the crest of a structure. This results in a modelling scenario where the injected fluids accumulate in the gas cap near the monitoring well, a scenario that is considerably more complex than a monitoring well that is not near a closed reservoir boundary.

All simulations in this section are performed using E7G, a version of the EOS7C module for the TOUGH2 simulator (Pruess, 1991) (Oldenburg et al., 2004). The domain is a dipping structure with a down-dip injection well and an up-dip monitoring well that are analogous to the CRC-1 and Naylor wells at Otway Stage 1. Reservoir simulation parameters used here are identical to those previously used (Jenkins et al., 2012) (LaForce et al, 2013). The only exceptions are that fluids are injected continuously for 1250 days, twice the real injection time in the field. The reason for the extended injection time is to continue to drive the second pulse of tracers past the monitoring well, rather than allowing them to flow past under buoyancy, as the change in drive mechanism would unnecessarily complicate the idealised models. Additionally both tracer pulses contain krypton, xenon, R134a, SF_6 and CD_4 and are injected during days 17 and 309.

Due to the observed sensitivity of tracer production profiles to numerical dispersion (LaForce et al., 2014) homogeneous, two-dimensional models are used exclusively in this study to allow for sufficient refinement of the simulation grid. LaForce et al (2014) observed that grid resolution had a large impact on the shape of tracer production curves. Simulations (not shown) indicate that the timing and the shape of tracer peaks may be impacted by numerical artefacts if the simulation grid is too coarse in the two-dimensional simulation. Initially a grid refinement study of both vertical and horizontal grid resolution was undertaken. Grids with 3, 6 10 and 20 *m* horizontal and 5, 2.5 and 1.667 *m* vertical resolution were considered. Little change in the tracer curves were observed between the most refined two vertical grids, while results were relatively insensitive to horizontal grid refinement. In any case, the finest simulation grid was chosen as this did not lead to prohibitive computation times. The final simulation grid has 3 *m* horizontal and 1.667 *m* vertical resolution and the simulation domain has total dimensions 25 × 25 × 610 *m*.

For Otway Stage 1 the reservoir domain is assumed to have a closed structure at the top so the injected gas will form a gas cap that fills downwards from the crest of the reservoir. Furthermore with the residual CH_4 saturation initially present, the mobilised CH_4 will continue to collect at the crest. It is pushed ahead of the injected CO_2 due to chromatographic separation as discussed in the previous section. CH_4 will remain above the CO_2 in the reservoir because it is a less dense fluid. In the case with a pre-existing CH_4 gas cap, the CH_4 will remain at the crest and the injected CO_2 or CO_2/CH_4 mixture will fill beneath the gas cap. There are two mechanisms where gas and tracers may reach a sampling depth in the observation well:

- Gas may enter the sampling point as a result of flow past the monitoring well as it travels up dip. In this case the analytical solutions in the preceding section should provide a rough intuition with regards to the expected tracer production profiles.
- Gas may reach the sampling depth by gas cap filling downward from the crest. In this case the gas and tracers may have mixed in the gas cap, in which case a low concentration of tracers will be sampled at gas breakthrough and there will be a very gradual decline in tracer concentration with increasing time due to mixing of fluids in the gas cap as injection continues. In this case all tracers will appear simultaneously with the gas and the analytical solutions in the preceding section may not provide intuition as to the expected tracer production profile.

There will likely not be a sharp transition between the two mechanisms, particularly in the case of a heterogeneous reservoir.

Three cases of increasing complexity are considered:

- Injection into an aquifer
- Injection into a gas field containing water and residual CH_4 gas
- Injection into a CH_4 field with a gas cap on the crest and residual CH_4 gas elsewhere.

For each initial reservoir condition, two injection mixtures are considered:

- Pure CO_2
- A mixture of 80% CO_2 and 20% CH_4.

It is beyond the scope of the present write-up to consider all six cases studied, so only two representative cases are shown: CO_2 injection into an aquifer and 80% CO_2/20% CH_4 mixed gas injection into a reservoir with a gas cap. The latter with mixed gas injection into a CH_4 field with a gas cap is most representative of the Otway stage 1 project.

3.2.1 CO_2 INJECTION INTO AN AQUIFER

Figure 25 shows the water saturation and concentration of SF_6 in the reservoir at two injection times for both the CO_2/water partition coefficients measured in this work and the literature air/water partition coefficients. SF_6 partition coefficients were chosen because this tracer had the largest difference between the air/water and supercritical CO_2/water partition coefficients, which have mass fraction basis coefficients of 1030 and 9.6, respectively.

SF_6 is the only tracer whose *in situ* concentration is visibly different for the two sets of partition coefficients. Even for SF_6, the difference in concentration is very minor. At breakthrough for U-tube 2, the first pulse of tracer, which has collected under the reservoir crest, is higher in the reservoir for the simulation with the air-water partition coefficients. The reason for this is that the air/water partition coefficient for SF_6 is much higher than the measured value in the laboratory. Hence the tracer reaches the reservoir boundary more quickly, when less of the crest of the reservoir has been filled.

Figure 26 shows the simulated production profiles in the two shallower U-tubes, U-tube 1 (left) and U-tube 2 (right) in the Naylor monitoring well as a function of time for all the tracers with air/water (top) and CO_2/water (bottom) partition coefficients. The simulated profiles in U-tube 3 (not shown) are qualitatively similar to U-tube 2, though the produced concentration is lower.

As there is no residual gas to mobilise in this simulation, it is anticipated that the simulations for $CD_{4,pure}$ and all the air/water tracers except R134a will show tracer arrival just prior to the injected CO_2 and at a high concentration relative to the injected concentration of 2×10^{-3} for all

the tracers. The production curves for U-tube 1 do not follow the expected trend with the tracers arriving after CO_2 breakthrough. This is because the gas containing the initial pulse of tracers in gas has flowed at a shallow depth and over the top of the U-tube and then diffuses downward as the gas cap fills in the aquifer. The large tracer peaks seen in U-tubes 1 and 2 in Figure 26 are from the second pulse of tracers injected for all the partition coefficients, as can be seen from location of the tracers in the reservoir in Figure 25. The tracers all arrive with the injected CO_2 at U-tubes 2 and 3.

Overall there is little separation of the tracers in the production curves, though they do follow the trend of a later peak production time with decreasing partition coefficient, as predicted by the analytical theory. For the laboratory coefficients, the first tracer to appear in U tube 1 is CD_4, because it has the largest partitioning into the gas phase. For the literature partition coefficients all the tracers arrive nearly simultaneously, with a slight lag in the R134a peak relative to the other tracers, because it had the smallest partition coefficient.

Nevertheless, all the simulation results are quite similar. The tracers all appear as a narrow peak of high concentration followed by a sharp drop off, with the highest partition coefficient tracers having the highest peaks. The peak concentration for all the tracers is higher than the injected concentration. This is in agreement with predictions from case 2 of the analytical solutions above for tracers with large partition coefficients which included the air/water coefficients except $R134a_{aw}$ and also the $CD_{4,pure}$ laboratory coefficient. However, for the other tracer partition coefficients the predicted displacement was included in case 1, with a later breakthrough and lower concentrations. This result is inconsistent with the case 1 analytical solutions. This is likely caused by the small difference between the CO_2 partition coefficient, which range from 22 to 44 and the tracer coefficients which range from 9.6 to 22.

In order to validate the analytical theory, flow-past simulations in which the reservoir was unbounded at the crest so there was no accumulation of gas were conducted (not shown). In that case the tracers were only detected at the shallowest point in the reservoir, and the expected chromatographic separation of tracers, CO_2 and CH_4 was observed. Thus, even in the case of a simple aquifer, the closed boundary at the crest has limited the separation of the tracers and complicated the interpretation of the displacement.

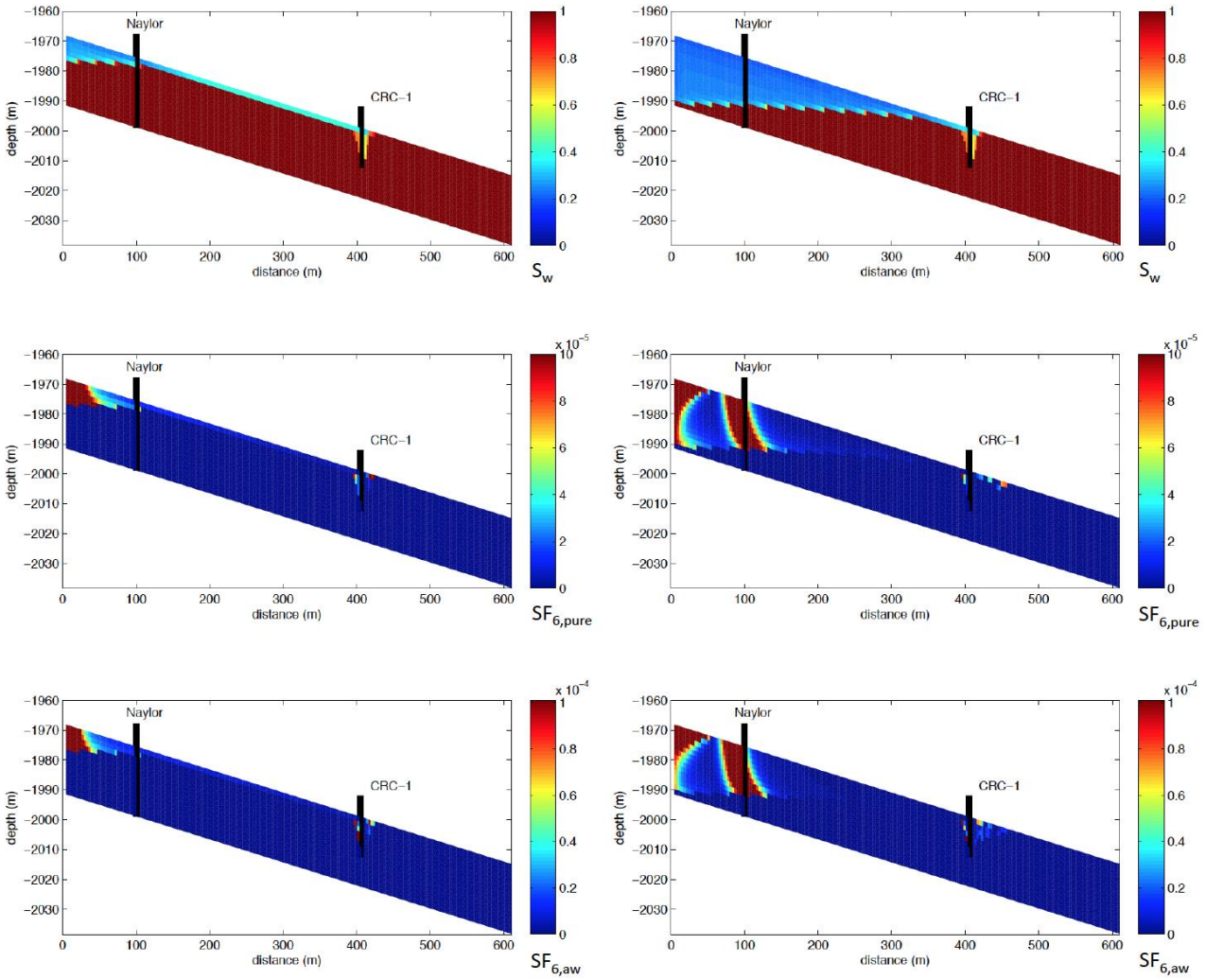

Figure 25 Tracers in the reservoir for injection of pure CO_2 into an aquifer originally containing no gas shortly before injected gas is observed at U tubes 1 and 2: 177 (left), and 704 (right) days: from the top: S_w, $SF_{6,pure}$, and $SF_{6,aw}$.

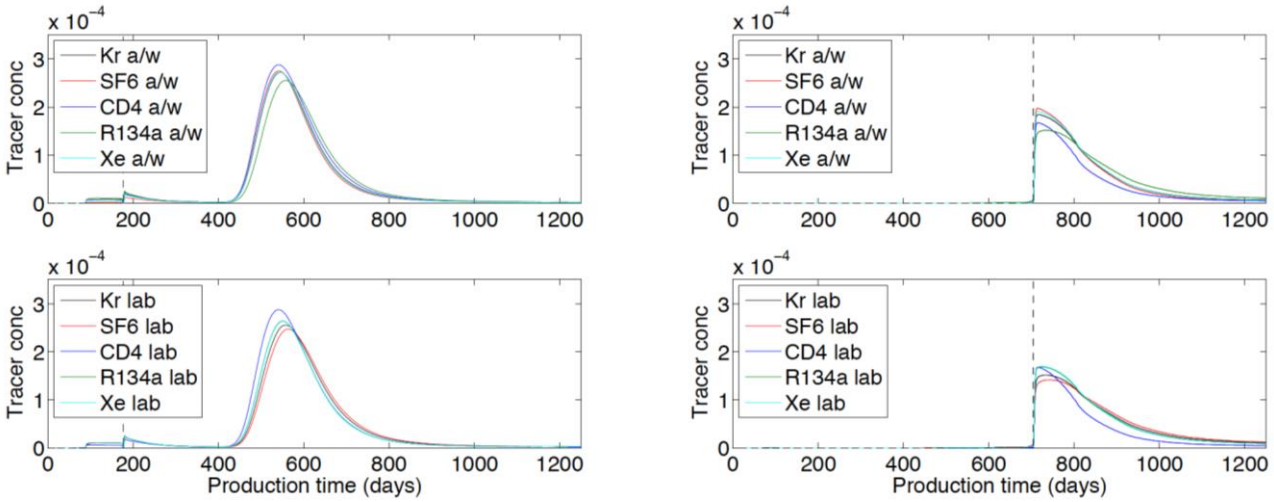

Figure 26 Tracer production profiles for injection of pure CO_2 into an aquifer originally containing no gas. The two sampling points are U-tube 1 (left) and U-tube 2 (right). Tracer production curves for air/water partition are in the top subfigures, while measured CO_2/water partition coefficients are in the bottom subfigures. Dashed line indicates breakthrough of injected gas at the observation point.

3.2.2 MIXED 80% CO_2/20% CH_4 INJECTION INTO A FIELD WITH A GAS CAP

The simulation results are shown in Figure 27 for the water saturation, CO_2 concentration in the gas phase, and concentration of SF_6 in the reservoir at two injection times for both the air/water and mixed CO_2-CH_4/water partition coefficients. Similar to Figure 25, SF_6 was chosen here because the two K-values are broadly representative of the changes in partitioning behaviour for all of the tracers. Much like the aquifer example, there is very little difference in the *in situ* distribution of tracers for the air/water vs CO_2-CH_4/water partition coefficients. The tracer pulse is slightly less dispersed for the higher air/water coefficient, but the concentration plots are otherwise extremely similar.

Figure 28 shows the produced tracer profiles at the two deeper U-tubes in the Naylor monitoring well as a function of time for all the tracers and partition coefficients. In this example, U-tube 1 is in the pre-injection CH_4 gas cap similarly to the Otway Stage 1 field trial. Due to the higher density of CO_2 relative to CH_4, the CO_2 collects underneath the pre-existing CH_4 gas cap for this homogeneous simulation domain, as can be seen in the CO_2 plots in Figure 27. As the tracers are travelling with the injected gases, tracer is never observed at U-tube 1 in the simulations.

Comparison of Figure 26 and Figure 28 shows that the shape of the tracer pulse in the reservoir is very different between the two cases. The spreading of the injected gas beneath the gas cap has resulted in spread of the tracers beneath the gas cap. The first tracer pulse is seen in U-tubes 2 and 3 because of the much earlier gas breakthrough time, as can be seen in Figure 27 and Figure 28. The second pulse of tracers is never observed in the U-tubes because it remains lower in the reservoir than the monitoring points. The peak tracer concentration at U-tube 2 is much higher than the injected concentration because the tracer has flowed past the sampling depth just after gas breakthrough, before they have dispersed along the bottom of the gas cap. The spreading of the tracers beneath the gas cap means that only low concentrations of tracers will reach U-tube 3.

Based on the analytical solutions, all the tracer simulations except $R134a_{80/20}$ are expected to show tracer arrival after the mobilised CH_4, and just before or at the same time as the injected CO_2. Figure 28 shows that this is indeedd the case for U-tube 2, where the tracers all appear

shortly after gas breakthrough, with a slightly later and lower peak for R134a$_{aw}$. Once again the tracers show slight some chromatographic separation by partition coefficient, with higher partition coefficient tracers peaking earlier. In U-tube 3 all the tracers appear simultaneously with the injected gas and there is little separation of the tracers.

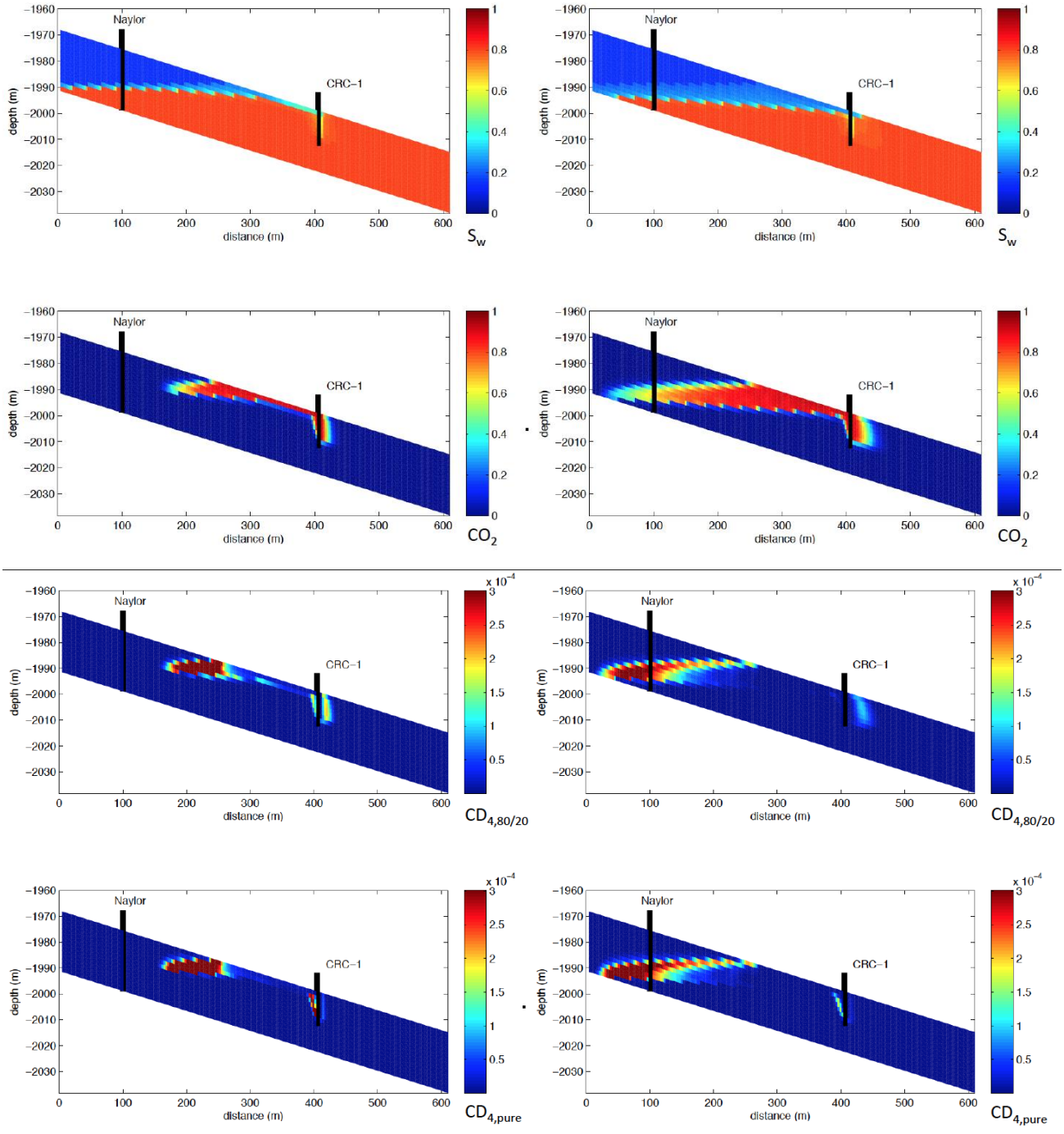

Figure 27 Tracers in the reservoir for injection of mixed 80% CO_2 and 20% CH_4 into a depleted reservoir with a gas cap shortly before injected gas is detected at U tubes 2 and 3: 156 (left), and 303 (right) days: from the top: S_w, CO_2, $SF_{6,80/20}$, and $SF_{6,aw}$.

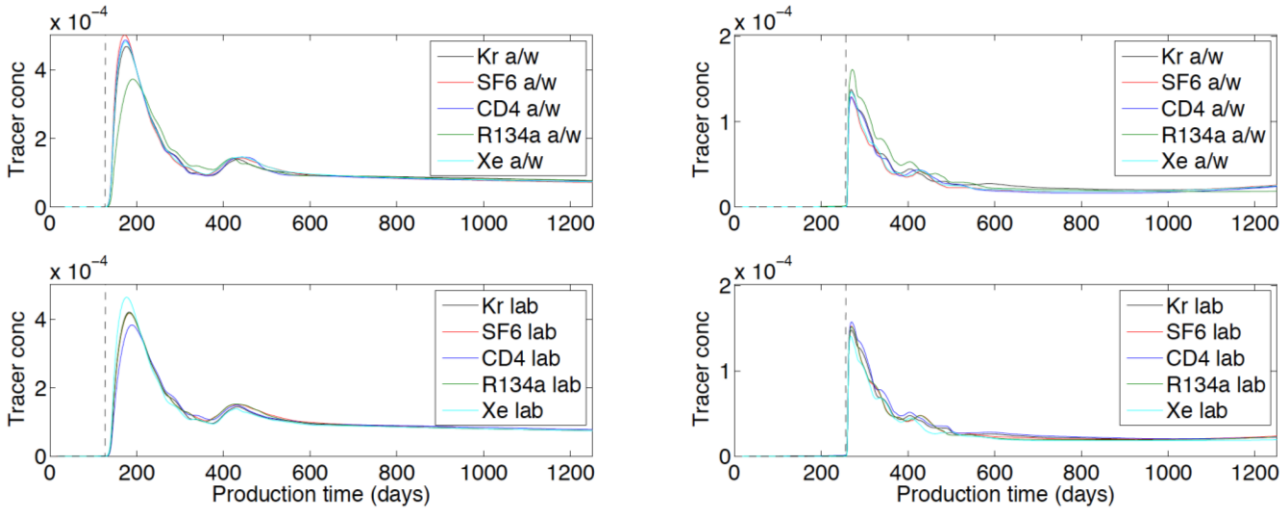

Figure 28 Tracer production profiles for mixed 80% CO_2 and 20% CH_4 injection into a depleted reservoir with a gas cap. The two sampling points are U-tube 2 (left) and U-tube 3 (right). Tracer production curves for air/water partition coefficients from the literature are in the top subfigures, while the measured laboratory partition coefficients are in the bottom subfigures. Dashed line indicates breakthrough of injected gas at the observation well.

3.2.3 TWO-DIMENSIONAL SIMULATION RESULTS

The supercritical CO_2/water coefficients are lower than their corresponding air/water partition coefficients, with the exception of R134a. However, the impact of the new partition coefficients on produced tracer at monitoring points and *in situ* distribution in the reservoir is small. The existence of a pre-existing gas cap and mixed gas injection at the Otway site added considerable complexity to interpretation of the results, even though simulations were still greatly simplified from the real field test.

The analytical solutions in the preceding section were qualitatively correct in predicting the relative time that tracers would appear with respect to each other for all tracers. In one case the analytical solutions also predicted the arrival time of tracers relative to the injected fluid. However in several cases, the injected gas reached the monitoring well when there was little tracer present due to the injection of tracers in two pulses. In these cases, the tracers can arrive either earlier or later than predicted by the analytical theory.

3.3 Conclusions

Overall these simulations highlight the considerable complexity that is introduced in moving from analytical models to reservoir simulations, even in a highly idealised simulation setting. Though the new CO_2/water partition coefficients are often quite different than the air/water literature values, the changes in the shape and timing of the tracer production curves would be extremely difficult to detect in field measurements where the reservoir boundary and initial fluid composition also impact the movement of tracers.

In the one-dimensional analytical solutions the new tracer partition coefficients resulted in a fundamental shift in the expected arrival time of many of the tracers relative to the CH_4 and CO_2. If multiple tracers were injected at once, the chromatographic separation of the tracer peaks was discernible for the air/water, pure CO_2/water, and 80% CO_2/20% CH_4 partition coefficients.

Simplified two-dimensional simulations of CO_2 or CO_2/CH_4 injection with an up-dip a monitoring well near the reservoir boundary were run. Initially a grid-refinement analysis was undertaken to verify that changes in tracer peak shape and breakthrough time were not impacted by numerical error. In the simulations, the new partition coefficients did not greatly change the expected tracer production profiles, other than ordering of peaks if multiple tracers were injected simultaneously. However, the chromatographic separation of peaks predicted by the analytical solutions was small and it would be very difficult to interpret even with a modest amount of scatter in field data.

One way to establish the correct relative arrival times of the CH_4, CO_2 and tracers in a general porous media setting would be to perform slim tube or core flood experiments with continuous tracer injection. Qualitative results would be immediately obvious from measured effluents. Fully quantitative analytical solutions including volume-change on mixing could also be used to predict the partition coefficients from slim-tube experiments.

4 Implications for reservoir modelling of Otway Stage 1

The simplified simulation of the Otway Stage 1 project above results in the predicted tracer arrival at the monitoring points U-tube 2 and 3 nearly simultaneously with the injected gas, and also results in little chromatographic separation of the tracers. The field tracer production data from U-tubes 2 and 3 in the Naylor well in the Otway stage 1 project is shown in Figure 29. A thorough analysis of the tracer data is discussed in Stalker et al. (in prep.) and only the aspects relevant to the simulations are briefly summarised here. The peak in CD_4 at U-tubes 2 and 3 were observed to be considerably later than the peaks for SF_6 and Kr. SF_6 and Kr also achieved maximum concentration prior to detection of the supercritical CO2 phase; however, this was well after the arrival of dissolved CO_2.

Thus there is an indication of separation of the tracers in the field, which may be caused by chromatographic affects discussed in this work, or may be the result of other physical mechanisms, such as tracer adsorption or differing flow paths through the reservoir. There is no way to determine whether the tracers pass the U-tubes as a result of flow-past or reservoir filling down from the gas cap. Nonetheless, the separation of tracers will likely prove to be a key insight into the full interpretation of the tracer data in the field.

A detailed history-match was done on all available data from the start of commercial reservoir production from the Naylor well to the end of the Stage 1 project in Ennis-King et al (2011) and Jenkins et al (2012). Geological models were based on seismic data, core analysis and well logs. Well rates, pressures and produced fluid ratios were matched to the Stage 1 data. An excellent fit of the simulations to SF_6 and CO_2 production at U-tube 2 was achieved, along with an acceptable fit to the U-tube 3 data in Ennis-King et al (2011). In order to match the U-tube 1 data it was necessary to run a simplified 2D model with a hypothesised permeability barrier in place that gave the tracers a different travel path through the reservoir to U-tube 1 compared to the other U-tubes.

Any comparison of the field data and the simulated models in this work can only be qualitative because of the large number of factors left out of the simulated model.

1. Clearly heterogeneity is an important factor left out of the model, as it was impossible to match the data in U-tube 1 without including the low-permeability barrier near the well. (Ennis-King et al, 2011; Jenkins et al, 2012)
2. The rate of gas-cap filling is also not likely to be accurately reproduced by any two-dimensional model, due to the difference in geometry between the actual boundaries of the fault block and the square sides of a 2D simulation domain.
3. Some other physical mechanisms not accounted for in this simulation study are:
    a. potential loss of SF_6 or other tracers due to adsorption onto sediment,
    b. relative permeability hysteresis, (studied in Ennis-King et al, 2011)
    c. pockets of mobile gas in the reservoir due to poor sweep during primary reservoir depletion,
    d. impact of small amounts of heavier hydrocarbons in the reservoir and injection gas.

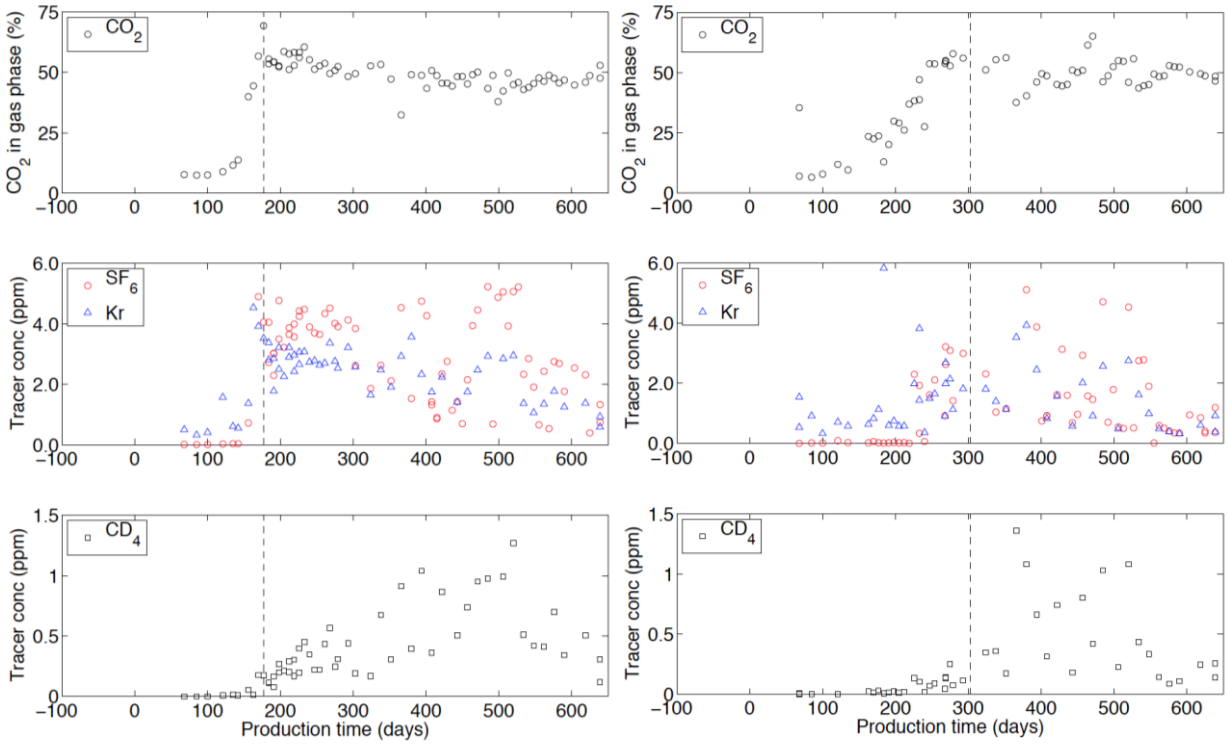

Figure 29 Tracer production profiles observed in Naylor well at U-tube 2 (left) and U-tube 3 (right). The measured evolved gas compositions are symbols. The dashed lines show the transition to self-lifting gas in the U-tubes. Injected gas arrives at the sampling point sometime prior to self-lift.

4.1.1 COMPARISON OF SIMULATED AND FIELD TRACER PROFILES FOR U-TUBE 1

In the two-dimensional, homogeneous model in this work, no tracer or CO_2 were observed in U-tube 1 for the simulations most representative of the Otway stage 1 project. This result is not consistent with the field data, or the current understanding of the heterogeneity of the reservoir at the Naylor well near U-tube 1 (Ennis-King et al, 2011; Jenkins et al., 2012). The reason for this is that the idealised model in the current work does not contain the heterogeneity from the field-specific simulations in the earlier work.

4.1.2 COMPARISON OF SIMULATED AND FIELD TRACER PROFILES FOR U-TUBE 2

For the purposes of comparison, in Figure 30, the SF_6, Kr and CD_4 field data for U-tube 2 are normalised to have the same area under the curve and plotted on the same axes as the homogeneous, two-dimensional simulations. The injection rate in the simulations was scaled to have the correct CO_2 breakthrough time in U-tube 2 resulting in the excellent agreement between the simulated and field CO_2 curves in the top subfigures of Figure 30. Due to mixing caused by heterogeneity, three-dimensional flow, and other physics in the reservoir the observed CO_2 concentration is always lower than predicted by the simulation model.

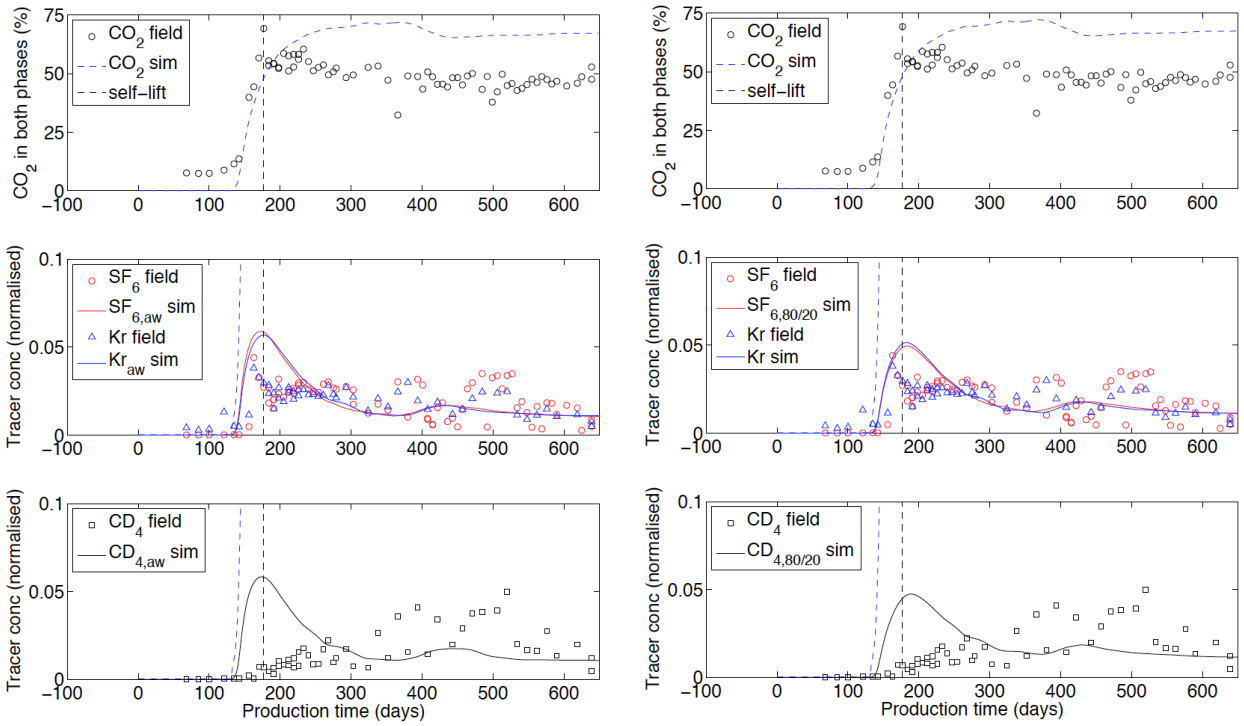

Figure 30 Qualitative comparison of CO_2 and tracer production curves at U-tube 2. Simulated results from two-dimensional homogeneous model are shown as solid lines while scaled field data are symbols. Left: Simulations with air/water partition coefficient. Right: Simulations with supercritical CO_2-CH_4/water partition coefficients from the current study. Top: CO_2 in the gas phase; middle: SF_6 and Kr tracer curves; bottom: CD_4 tracer curves.

Though the fit to the shape of the field tracer curves is difficult to determine due to scatter in the data, SF_6 and Kr peak just prior to self-lift of the supercritical CO_2 phase in U-tube 2, while CD_4 peaks around 300 days later (Stalker et al., *in prep*). The simulations with the air/water and CO_2-CH_4/water partition coefficients both predict the time of the peak in the SF_6 and Kr curves quite well, and miss the CD_4 tracer peak badly. From the previous section, the simultaneous breakthrough of tracer and CO_2 can be explained by either a high tracer partitioning coefficient or the gas cap moving downward past the U-tube sampling point when there is a high concentration of tracer in the gas phase.

Generally speaking, the simulations with the CO_2-CH_4/water partition coefficients have slightly later and more dispersed peaks than those with the air/water coefficients. This is a better match to the SF_6 and Kr field data than the air/water partition coefficients. However it is unclear if this is because the lower laboratory partition coefficients are more accurate, or because of dispersion in the reservoir. Simulations were also run with 5 and 10 vertical layers (not shown), and the increased vertical mixing due to the coarser grid also resulted in lower and more dispersed tracer peaks. The coarsest model peaks were considerably later than observed in the field for SF_6 and Kr, but matched the shape and timing of the CD_4 peak reasonably well. This result lends weight to the theory that in the field experiment CD_4 travelled to the U-tubes via a different path through the reservoir, which led to greater dispersion for this tracer.

4.1.3 COMPARISON OF SIMULATED AND FIELD TRACER PROFILES FOR U-TUBE 3

Figure 31 also shows the comparison of the simulated and field CO_2 and tracer profiles at U-tube 3. The tracer concentrations have again been scaled to have the same integrated. Due to the

heterogeneity in the field, and possibly communication between the two sampling points at U-tube 2 and U-tube 3, the breakthrough of CO_2 and tracers at U-tube 3 is not well predicted by the homogeneous simulations. Similar to U-tube 2, the predicted CO_2 concentration is higher than observed in the field data and likely due to mixing in the field.

In this case, the scatter in the field data makes it very difficult to tell which simulation may be more accurate in modelling the data. All the simulations have simultaneous breakthrough of dissolved CO_2, SF_6 and Kr tracers due to downward filling from the gas cap, which does appear to be consistent with the field data. The high peak in tracer concentration predicted by the simulations is not observed in the data, rather a low production of tracers of a long time is observed. Once again the late arrival of CD_4 is not predicted in the simulated production curves.

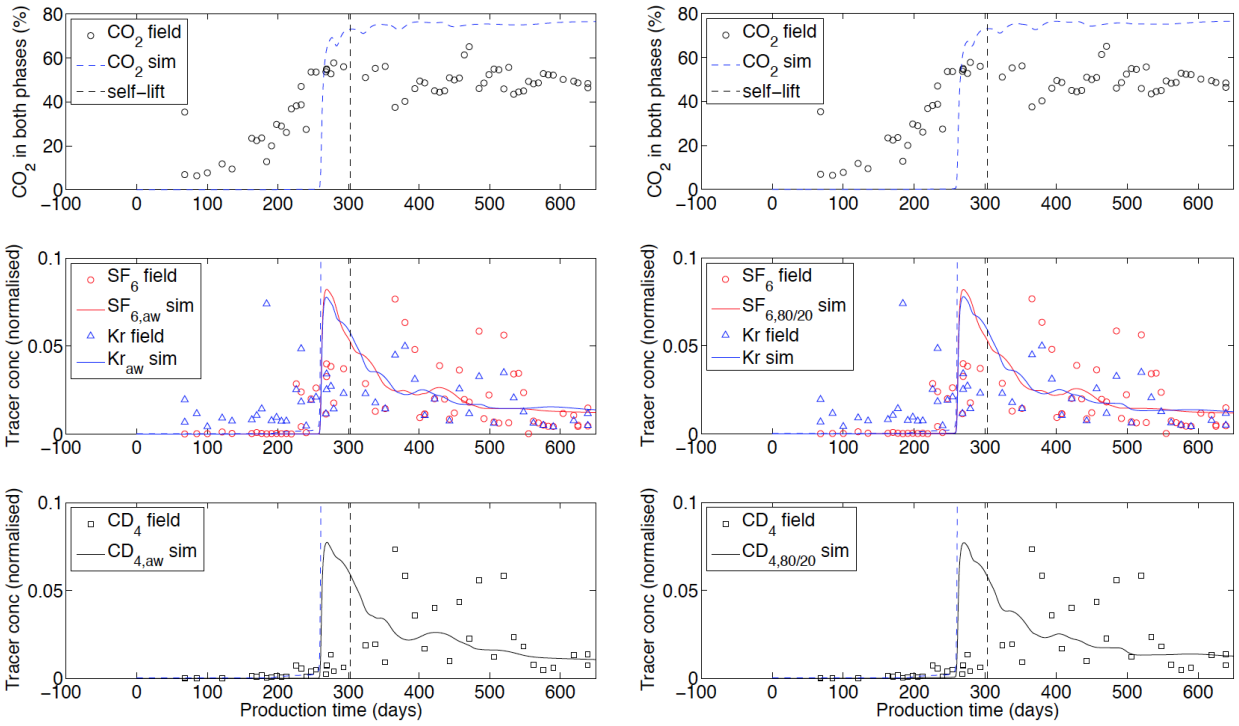

Figure 31 Qualitative comparison of CO_2 and tracer production curves at U-tube 3. Simulated results from two-dimensional homogeneous model are shown as solid lines while scaled field data are symbols. Left: Simulations with air/water partition coefficient. Right: Simulations with CO_2-CH_4/water partition coefficients from the current study. Top: CO_2 in the gas phase; middle: SF_6 and Kr tracer curves; bottom: CD_4 tracer curves.

4.2 Conclusions

The simulated tracer peaks are much higher and narrower than was observed in the field data for SF_6 and Kr. This is likely due to field heterogeneity in the field that was not included in the models. The simulated production curves for CD_4 did not predict the field displacement at all, though a very high dispersion simulation was better able to model the CD_4 field data.

Based on the simulated results, breakthrough at U-tube 2 is expected to be nearly simultaneous for all the tracers. The tracers are expected to appear just after arrival of the mobile CO_2 phase. In the field data, SF_6 and Kr are indeed observed in U-tube 2 prior to arrival of the supercritical CO_2 phase and after the arrival of dissolved CO_2. High initial concentration is anticipated with a rapid decrease after CO_2 breakthrough to a lower concentration, which is also observed in the field data.

Tracer production curves at U-tube 3 were expected to show little separation in the tracer peaks and to appear simultaneously with the mobile CO_2 then rapidly decline. In the field data the SF_6 and Kr tracers appeared simultaneously with dissolved CO_2 and prior to the detection of the mobile CO_2 phase, but there is no sharp decline in tracer concentration.

The simplified simulations used here to discern the impact of the tracer partition coefficients on the tracer behaviour are not tailored to the detailed geology of the Otway site, and as such can only show general trends that will apply to fields with a monitoring well near a trap. Specialised simulations must be run for each field to have predictive simulations. Substantial progress on history matching the Otway stage 1 data using the air/water partition coefficients has been made and is continuing with the additional data acquired as part of the current work. (Ennis-King et al, 2011; Jenkins et al., 2012).

Finally the tracer curves from the simplified simulation model were qualitatively compared with the measured concentrations at the Naylor monitoring well during the Otway stage 1 project. In U-tubes 2 and 3, the SF_6 and Kr tracers appeared simultaneously with the dissolved CO_2 and before the mobile CO_2 phase, which is broadly consistent with the simulated result. In U-tube 2, SF_6 and Kr also had a rapid peak and decline in concentration, which is consistent with the simulations. In U-tube 3 the simulated results did not accurately predict the shape of the tracer curves for any of the tracers.

We intend to continue the data-fitting process that was started in Ennis-King et al (2011) and Jenkins et al. (2012) to see if a better match to the field data can be attained. The partition coefficients and general simulation results for an 'Otway 1 like' reservoir setting in this work will be invaluable to continuing this research.

Part VI References

Atlan, S., Trelea, I.C., Saint-Eve, A., Souchon, I. and Latrille, E., 2006. Processing Gas Chromatographic Data and Confidence Interval Calculation for Partition Coefficients Determined by the Phase Ratio Variation Method. Journal of Chromatography A, 1110(1-2): 146-155.

Bahadur, N.P., Shiu, W.-Y., Boocock, D.G.B. and Mackay, D., 1997. Temperature Dependence of Octanol−Water Partition Coefficient for Selected Chlorobenzenes. Journal of Chemical & Engineering Data, 42(4): 685-688.

Boreham, C. et al., 2011. Monitoring of CO_2 Storage in a Depleted Natural Gas Reservoir: Gas Geochemistry from the CO2CRC Otway Project, Australia. International Journal of Greenhouse Gas Control, 5(4): 1039-1054.

Cronin, M.T.D. et al., 2003. Use of QSARs in International Decision-Making Frameworks to Predict Ecologic Effects and Environmental Fate of Chemical Substances. Environmental Health Perspectives, 111(10): 1376-1390.

Ennis-King, J., Dance, T., Xu, J., Boreham C., Freifeld B., Jenkins C., Paterson L., Sharma S., Stalker L., Underschultz, J., 2011. The role of heterogeneity in CO_2 storage in a depleted gas field: history matching of simulation models to field data for the CO2CRC Otway Project, Australia, Energy Procedia 4: 3494-3501.

Fredenslund, A., Jones, R.L. and Prausnitz, J.M., 1975. Group-Contribution Estimation of Activity-Coefficients in Nonideal Liquid-Mixtures. Aiche Journal, 21(6): 1086-1099.

Freifeld, B.M. et al., 2005. The U-Tube: A Novel System for Acquiring Borehole Fluid Samples from a Deep Geologic CO_2 Sequestration Experiment. Journal of Geophysical Research-Solid Earth, 110(B10).

Gomes, M.F.C. and Grolier, J.P., 2001. Determination of Henry's Law Constants for Aqueous Solutions of Tetradeuteriomethane between 285 and 325 K and Calculation of the H/D Isotope Effect. Physical Chemistry Chemical Physics, 3(6): 1047-1052.

Gossett, J.M., 1987. Measurement of Henry's Law Constants for C1 and C2 Chlorinated Hydrocarbons. Environmental Science & Technology, 21(2): 202-208.

Hansen, K.C., Zhou, Z., Yaws, C.L. and Aminabhavi, T.M., 1993. Determination of Henry's Law Constants of Organics in Dilute Aqueous Solutions. Journal of Chemical & Engineering Data, 38(4): 546-550.

Haynes, W.M. (Editor), 2011. Crc Handbook of Chemistry and Physics. CRC Press/Taylor and Francis, Boca Raton, FL.

Hovorka, S.D. et al., 2006. Measuring Permanence of CO_2 Storage in Saline Formations: The Frio Experiment. Environmental Geosciences, 13(2): 105-121.

Jenkins, C.R. Cook, P.J., Ennis-King, J., Undershultz, J., Boreham, C., Dance, T., de Caritat, P., Etheridge, D.M., Freifeld, B.M., Hortle, A., Kirste, D., Paterson, L., Pevzner, R., Schacht, U., Sharma, S., Stalker, L., and Urosevic, M., 2012. Safe Storage and Effective Monitoring of CO_2 in Depleted Gas Fields. Proceedings of the National Academy of Sciences, 109(2): E35-E41.

Lau, K., Rogers, T.N. and Chesney, D.J., 2010. Measuring the Aqueous Henry's Law Constant at Elevated Temperatures Using an Extended EPICS Technique. Journal of Chemical and Engineering Data, 55(11): 5144-5148.

LaForce, T. Ennis-King, J., and Paterson, L., 2013. Magnitude and duration of temperature changes in geological storage of carbon dioxide. *Energy Procedia. 37*, pp. 4465-4472. Kyoto, Japan: Elsevier.

LaForce, T., et al., 2014. Residual CO_2 saturation estimate using noble gas tracers in a single-well field test: The CO2CRC Otway project. *International Journal of Greenhouse Gas Control* 26, 9-21 .

Magnussen, T., Rasmussen, P. and Fredenslund, A., 1981. Unifac Parameter Table for Prediction of Liquid-Liquid Equilibria. Industrial & Engineering Chemistry Process Design and Development, 20(2): 331-339.

Moreira, L.A., Oliveira, F.A.R., Silva, T.R. and Oliveira, J.C., 1993. Development of a Non-Isothermal Method for Determination of Diffusional Parameters. International Journal of Food Science & Technology, 28(6): 575-586.

Mroczek, E.K., 1997. Henry's Law Constants and Distribution Coefficients of Sulfur Hexafluoride in Water from 25 °C to 230 °C. Journal of Chemical & Engineering Data, 42(1): 116-119.

Myers, M., Stalker, L., Pejcic, B. and Ross, A., 2012a. Tracers - Past, Present and Future Application in Co_2 Geosequestration. Applied Geochemistry: in press.

Myers, M., Stalker, L., Ross, A., Dyt, C. and Ho, K.-B., 2012b. Method for the Determination of Residual Carbon Dioxide Saturation Using Reactive Ester Tracers. Applied Geochemistry: in press.

Myers, M., Stalker, L., Ross, A., Dyt, C. and Ho, K.-B., 2012c. Method for the Determination of Residual Carbon Dioxide Saturation Using Reactive Ester Tracers. Applied Geochemistry, 27(10): 2148-2156.

Oldenburg, C.M., Moridis, G.J., Spycher, N.F. and Pruess, K., 2004. EOS7c Version 1.0: TOUGH2 Module for Carbon Dioxide or Nitrogen in Natural Gas (Methane) Reservoirs, Lawrence Berkeley National Laboratory, Berkeley, CA

Orr, J. F. (2007). *Theory of gas injection processes.* Holte, Denmark: Tie-Line Publications.

Paterson, L. Boreham, C., Bunch, M., Dance, T., Ennis-King, J., Freifeld, B., Haese, R., Jenkins, C., LaForce, T., Raab, M., Singh, R., Stalker, L. and Zhang, Y. 2013. Overview of the CO2CRC Otway Residual Saturation and Dissolution Test. Energy Procedia, 37(0): 6140-6148.

Paterson, L. et al., 2010. The CO2CRC Otway Stage 2b Residual Saturation and Dissolution Test.

Pruess, K. (1991). *TOUGH 2-A general-purpose numerical simulator for multiphase fluid and heat flow.* Berkeley, CA, USA: LBNL.

Ramachandran, B.R., Allen, J.M. and Halpern, A.M., 1996. The Importance of Weighted Regression Analysis in the Determination of Henry's Law Constants by Static Headspace Gas Chromatography. Analytical Chemistry, 68(2): 281-286.

Rathbun, R.E., 2000. Transport, Behavior, and Fate of Volatile Organic Compounds in Streams. Critical Reviews in Environmental Science and Technology, 30(2): 129-295.

Renner, R., 2002. The Kow Controversy. Environmental Science & Technology, 36(21): 410A-413A.

Robbins, G.A., Wang, S. and Stuart, J.D., 1993. Using the Static Headspace Method to Determine Henry's Law Constants. Analytical Chemistry, 65(21): 3113-3118.

Srebrenik, S. and Cohen, S., 1976. Theoretical Derivation of Partition Coefficient from Solubility Parameters. The Journal of Physical Chemistry, 80(9): 996-999.

Stalker, L., Boreham, C., Underschultz, J., Freifeld, B., Perkins, E., Schacht, U., Sharma, S., *in preparation*. Application of tracers to measure, monitor and verify breakthrough of sequestered CO_2 at the CO2CRC Otway Project, Victoria, Australia, Chemical Geology XX: XX-XX

Strazisar, B.R., Wells, A.W., Diehl, J.R., Hammack, R.W. and Veloski, G.A., 2009. Near-Surface Monitoring for the Zert Shallow CO_2 Injection Project. International Journal of Greenhouse Gas Control, 3(6): 736-744.

Timko, M.T., Nicholson, B.F., Steinfeld, J.I., Smith, K.A. and Tester, J.W., 2004. Partition Coefficients of Organic Solutes between Supercritical Carbon Dioxide and Water: Experimental Measurements and Empirical Correlations. Journal of Chemical and Engineering Data, 49(4): 768-778.

Underschultz, J. et al., 2011. CO_2 Storage in a Depleted Gas Field: An Overview of the CO2CRC Otway Project and Initial Results. International Journal of Greenhouse Gas Control, 5(4): 922-932.

Vandeweijer, V. et al., 2011. Monitoring the CO_2 Injection Site: K12-B. Energy Procedia, 4(0): 5471-5478.

Wells, A., Strazisar, B., Diehl, J.R. and Veloski, G., 2010. Atmospheric Tracer Monitoring and Surface Plume Development at the Zert Pilot Test in Bozeman, Montana, USA. Environmental Earth Sciences, 60(2): 299-305.

Wells, A.W. et al., 2007. The Use of Tracers to Assess Leakage from the Sequestration of CO_2 in a Depleted Oil Reservoir, New Mexico, USA. Applied Geochemistry, 22(5): 996-1016.

Wilhelm, E., Battino, R. and Wilcock, R.J., 1977. Low-Pressure Solubility of Gases in Liquid Water. Chemical Reviews, 77(2): 219-262.

Zhang, Y. et al., 2011. Single-Well Experimental Design for Studying Residual Trapping of Supercritical Carbon Dioxide. International Journal of Greenhouse Gas Control, 5(1): 88-98.

Zheng, D.-Q., Guo, T.-M. and Knapp, H., 1997. Experimental and Modeling Studies on the Solubility of CO_2, $CHClF_2$, CHF_3, $C_2H_2F_4$ and $C_2H_4F_2$ in Water and Aqueous Nacl Solutions under Low Pressures. Fluid Phase Equilibria, 129(1–2): 197-209.

CONTACT US

t 1300 363 400
+61 3 9545 2176
e enquiries@csiro.au
w www.csiro.au

YOUR CSIRO

Australia is founding its future on science and innovation. Its national science agency, CSIRO, is a powerhouse of ideas, technologies and skills for building prosperity, growth, health and sustainability. It serves governments, industries, business and communities across the nation.

FOR FURTHER INFORMATION

Earth Science and Resource Engineering
Matthew Myers
t +61 8 6436 8708
e matt.myers@csiro.au